NASA CONTRACTOR REPORT

NASA CR-1563

DESIGN, FABRICATION AND TESTING OF A FOIL GAS-BEARING TEST RIG

by L. Licht

Prepared by
AMPEX CORPORATION
Redwood City, Calif.
for Lewis Research Center

NATIONAL AERONAUTICS AND SPACE ADMINISTRATION • WASHINGTON, D. C. • MAY 1970

1. Report No.	2. Government Accession No.	3. Recipient's Catalog No.
NASA CR-1563		

4. Title and Subtitle	5. Report Date
DESIGN, FABRICATION AND TESTING OF A FOIL GAS-BEARING TEST RIG	May 1970
	6. Performing Organization Code

7. Author(s)	8. Performing Organization Report No.
L. Licht	AMPEX-RR 69-9

9. Performing Organization Name and Address	10. Work Unit No.
Ampex Corporation 401 Broadway Redwood City, Calif. 94063	11. Contract or Grant No. NAS3-11826
	13. Type of Report and Period Covered Contractor Report
12. Sponsoring Agency Name and Address National Aeronautics and Space Administration Washington, D.C. 20546	14. Sponsoring Agency Code

15. Supplementary Notes

16. Abstract

A sixteen-inch long rotor, weighing approximately twenty-one pounds, was supported by air-lubricated foil bearings. In physical size and in mass distribution, the rotor was closely matched with that of an experimental Brayton cycle turbo-alternator unit. The rotor was stable in both the vertical and horizontal attitudes at speeds up to and in excess of 48,000 rpm. A detailed description of the experimental apparatus and of the foil bearing design are given. The report contains data of response of the rotor to rotating imbalance, symmetric and asymmetric, and to excitation by means of a vibrator (shake-table). It was demonstrated that the foil bearings accommodated thermal distortions and performed satisfactorily in the presence of appreciable temperature gradients along the journal. It is concluded that the gas-lubricated foil bearing suspension is stable and and that it is endowed with superior distortion-conforming and wear characteristics.

17. Key Words (Suggested by Author(s))	18. Distribution Statement
Turbomachinery Bearings Gas bearings	Unclassified - unlimited

19. Security Classif. (of this report)	20. Security Classif. (of this page)	21. No. of Pages	22. Price*
Unclassified	Unclassified	80	$3.00

*For sale by the Clearinghouse for Federal Scientific and Technical Information Springfield, Virginia 22151

FOREWORD

The work described herein, which was conducted by the Ampex Corporation in the Mechanics Section of the Research Department, was performed under NASA Contract NAS3-11826 and the technical management of William J. Anderson, Fluid System Components Division, NASA-Lewis Research Center.

CONTENTS

LIST OF FIGURES

---

* The scale μin/cm should be interpreted as microinches per division. The foregoing applies to all scales appended to oscilloscope photographs presented in this report.

1.0 INTRODUCTION

Foil bearings are generally associated with the transport of flexible webs under tension and, specifically, with the generation of lubricating films separating foil-like materials from arrays of cylindrical guides and rollers. Whether by design or by coincidence, foil bearings have always existed in the manufacture and processing of paper, plastic and metal foil, but recent studies of foil bearings received the impetus from the development of tape transports and of devices for magnetic recording on flexible media in general. A review of these studies is beyond the scope of the present investigation, and the reader is referred to comprehensive bibliographies contained in references [1] and [2].

With the exception of peripheral applications, such as loading devices, for example [3], no serious attempts have been made in the past to utilize foil bearings as actual supports for high-speed rotors. In the course of a recent feasibility study, however, speeds of the order 350,000 RPM were attained with a one pound, one inch diameter rotor, supported in the vertical attitude by very compliant foil bearings [4]. Rotation with preloaded foils could be initiated upon temporary flooding of bearings with liquid freon, but the experimenters found it difficult to control the foil suspension and the gyrations of the rotor.

The present study was facilitated by the results of an earlier investigation, reported in considerable detail in references [5] and [6]. The latter furnished useful results, applicable to the construction and the estimation of dynamic characteristics of the foil-bearing rotor support described in the following section. The objectives of the present study were to advance the foil-bearing concept from feasibility to practicality

as means of support for high-speed turbomachines and to increase the experience necessary for incorporation of the concept in a realistic design.

The mass and moment of inertia of the rotor were closely matched with those of an existing turbo-alternator and provision was made for rotation in both the vertical, that is radially unloaded, and in the horizontal attitudes. Experiments described in the following sections pertain to responses of the foil-rotor system in both attitudes. Data were obtained for rotation in both the pressurized and self-acting modes, with a balanced rotor and with various amounts of symmetric and asymmetric imbalance added. Additional information, relevant to the dynamic characteristics of the foil-bearing supported rotor, was derived from experiments involving excitations by means of a vibrator (shake-table).

An important aspect of this investigation was the study of effects of nonuniform heating on the performance of the foil bearings. Heat was supplied to a disc simulating the turbine wheel, and the thermal gradients induced in the adjacent journal and foils corresponded to rather extreme conditions anticipated under actual operating conditions.

2.0 DESIGN OF FOIL-BEARING SUSPENSION AND OF EXPERIMENTAL APPARATUS

Pictorial views of the foil-bearing supported rotor, in both the horizontal and vertical attitudes, are shown in Figs. 1 and 2. Component parts of the experimental apparatus are presented in greater detail in the photographs of Figs. 3, 4 and 5. In the description of the test apparatus, given in the following paragraphs, numbers in parentheses refer to components listed in the assembly drawing of Fig. 6 and in the schematic diagram of Fig. 7.

The 20.9 lb rotor (1) was 16 inches long and had a polar moment of inertia $I_p = 0.0595$ in-lb-sec^2 and a transverse moment of inertia $I_t = 1.185$ in-lb-sec^2. The rotor was symmetrical and details of the five-piece construction are illustrated in the drawing of Fig. 8. Two journal sleeves, 2.5 inches in diameter and approximately 4 inches long, were shrunk on the rotor core with a 0.002 inches interference fit at the 2 inch diameter interface. Each sleeve had 4 rows of 24 orifices, equally spaced along the periphery. Through these, compressed air was supplied from the interior of the rotor to separate the preloaded foils from the journals on starting, stopping, and at low rotational speeds. The location of orifice rows along the journals was 0.25 inches inboard from the edges of the 1.5 inch wide foils, arranged in tandem at each bearing journal.

Two end-discs, threaded into the core of the simulator, corresponded to the turbine and compressor wheels. For convenience, one of the discs was used as a thrust plate, through the center of which the hollow interior of the rotor was connected to the foil-lift pressure source. Provision was made for surrounding the second disc by a heating chamber for the purpose of simulating largely non-isothermal operating conditions.

Each disc contained 18 tapped holes for adding balancing screws. An air-driven turbine wheel (8), consisting of 24 milled buckets, was located at the center plane of the rotor. The entire rotor was made of AISI type 440C stainless steel, with journals hardened to C-56 Rockwell. The 2.5 inch diameter sleeves were concentric and round within 100 μinches, with taper the order of 50 μinches along the 4 inch journal lengths. The surface finish of journals was 4 μinches RMS.

The moments of inertia of the rotor were determined by pendulation within an accuracy of 2% and balancing was performed on a Schenck Balancing Machine, Model RS1-b to within 350 μinches in each balancing plane. The rotor and a lightweight balancing fixture, equipped with air-lubricated bearings, are shown in Fig. 3.

The foil bearings (2) were similar in construction to the experimental unit described in references [5] and [6]. Each foil-bearing support (3) contained clusters of symmetrically spaced guide posts (4) and foil locks (5), arranged in tandem on opposite sides of the support plates (3). The split-construction, doweled support plates were spaced 9 inches apart and securely assembled into a single frame. The 32 cantilevered foil guides, press-fitted in pairs into jig-bored holes and secured by means of tie bolts, were parallel to each other and to the reference planes of the foil-bearing support subassembly within 0.0002 inches.

The foil-bearing supports straddled a turbine nozzle-ring and manifold (9), from which 8 rectangular nozzles, operating at choked flow conditions, directed air jets, at an angle calculated to generate a relatively high torque at rated speed. Adjacent to the rotor ends were two precisely machined angle plates, the thrust bearing support plate (7) and the alignment support plate (16). The foil-bearing support assembly, the thrust-bearing support and the symmetrical alignment support, and the nozzle ring were securely bolted to a sturdy 1.5 x 12 x 26-inch aluminum

base (13), flat to within 0.002 inches. Spacing of the foregoing components was accomplished by means of precision gauge blocks and lateral alignment assured by using for reference a massive, precision-ground bar (10), attached to the base.

The construction of the fixed, externally pressurized thrust bearing (6) allowed for various adjustments and substitutions of components. While the investigation was focussed on the foil bearings, rather than on the thrust bearing, the operational clearances and outer dimensions of the latter were realistic and representative. The inboard thrust member consisted of three circular, axially adjustable pads, clamped on sturdy, cantilevered rods, pressed into the thrust-bearing support plate. This arrangement permitted a great deal of flexibility in adjusting the total axial clearance. The outboard thrust member consisted of a cluster of six circular and equally spaced pressure pads, which could be easily replaced by a single, multi-orifice plate.*

The annulus between a central pad and the rotating end disc provided a face seal for the foil-lift air supply, ducted through a 5/16 inch hole, concentric with the pad and the rotor axis. The seal was coplanar with the outboard thrust surface, but separated from the bearing areas and vented to the ambient atmosphere.

The inboard and outboard thrust members and the foil lift were supplied from separate and individually regulated plenums, located in the cover plate at the rear of the thrust-bearing support plate (7). The independently regulated supplies augmented the operational flexibility furnished by the adjustable thrust-bearing clearance. Details of thrust-bearing construction with a multi-orifice plate and 3 inboard pads are illustrated in Fig. 5.

*The outside diameters of the rotating disc, of the cluster of 6 pressure pads, and of the multi-orifice plate were respectively 3.25, 2.50 and 3.00 inches.

The procedure followed in securing and preloading of foils was the following: The rotor weight, supported initially on alignment pins (11) slip-fitted to matching holes in the rotor end discs and in the adjacent support plates, was counterbalanced by means of levers (12). The foils were then looped around the guides, brought into intimate contact with the journals along the upper arcs of wrap and secured at the outer posts of the upper guide-clusters. Preload weights were then attached to the free ends of the foils, threaded through guides adjacent to the foil locks. Upon removal of alignment pins, the foil bearings were pressurized and depressurized to equalize the preload tension in all three foil sectors prior to securing of foil locks. The counterbalancing of the rotor before preloading was convenient and equivalent to application of initial tension in the vertical attitude. In the last step, all weights were removed, making the simulator operational.

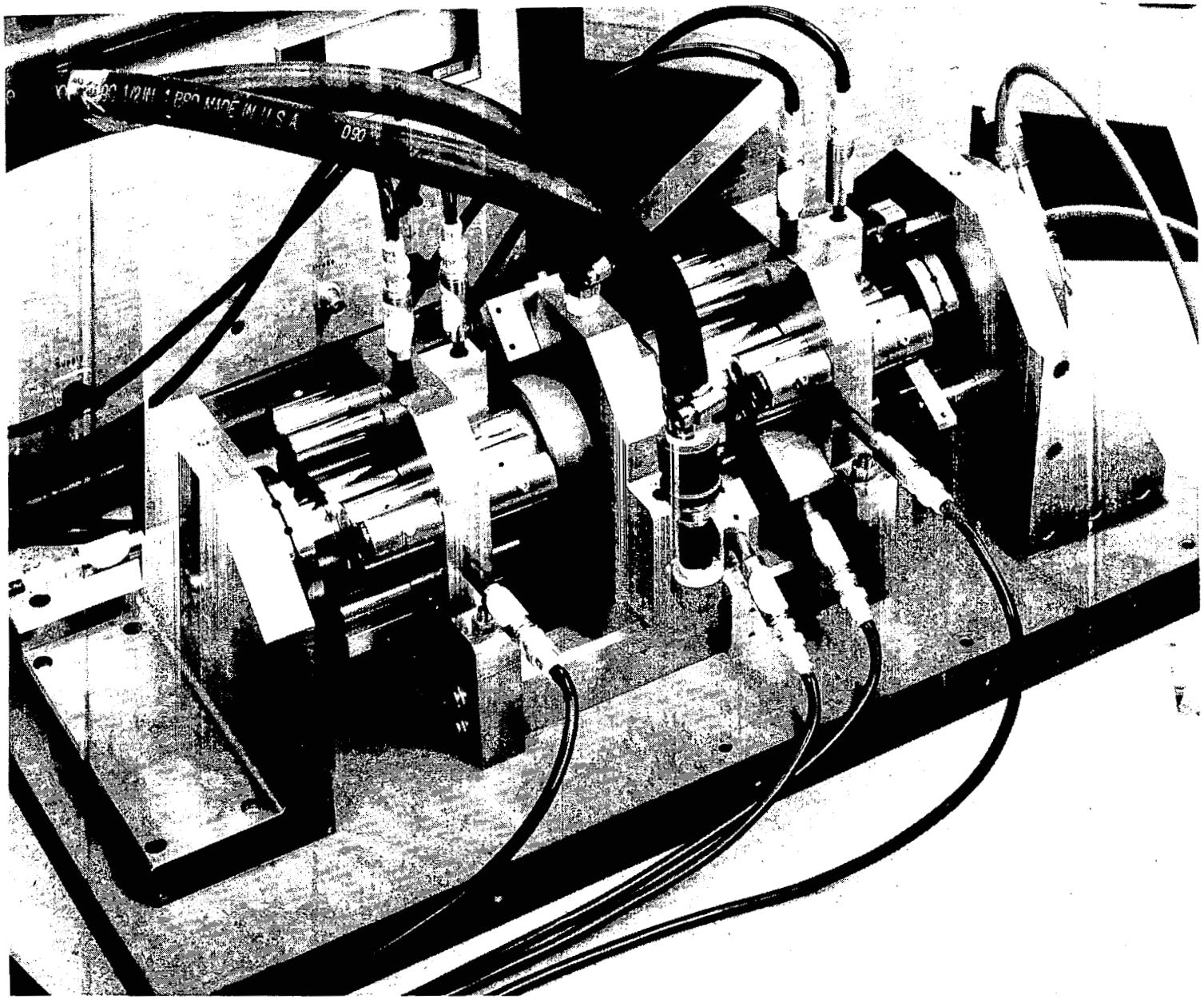

Fig. 1 View of Foil-Bearing Supported Rotor in the Horizontal Attitude

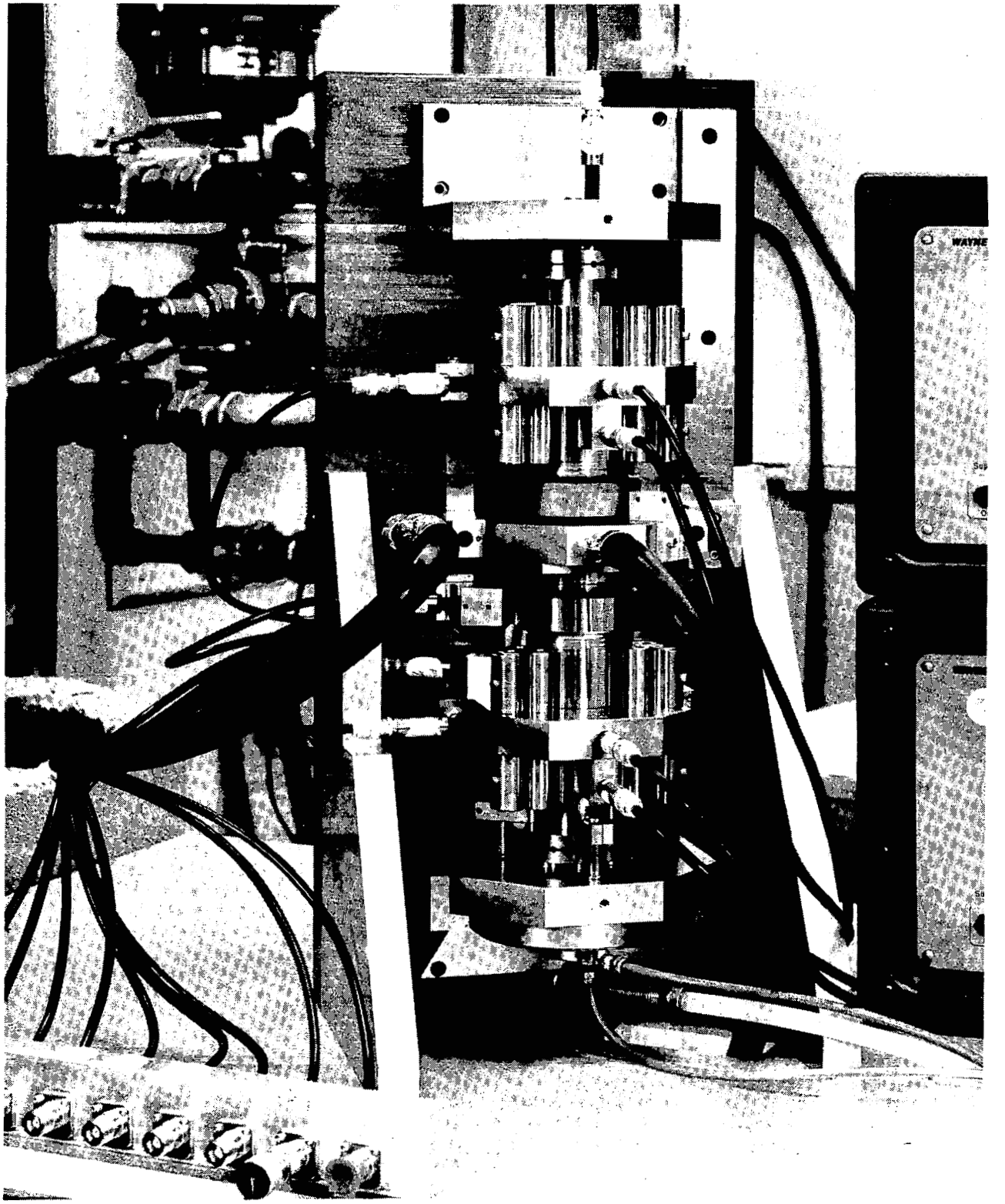

Fig. 2 View of Foil Bearing Supported in the Vertical Attitude

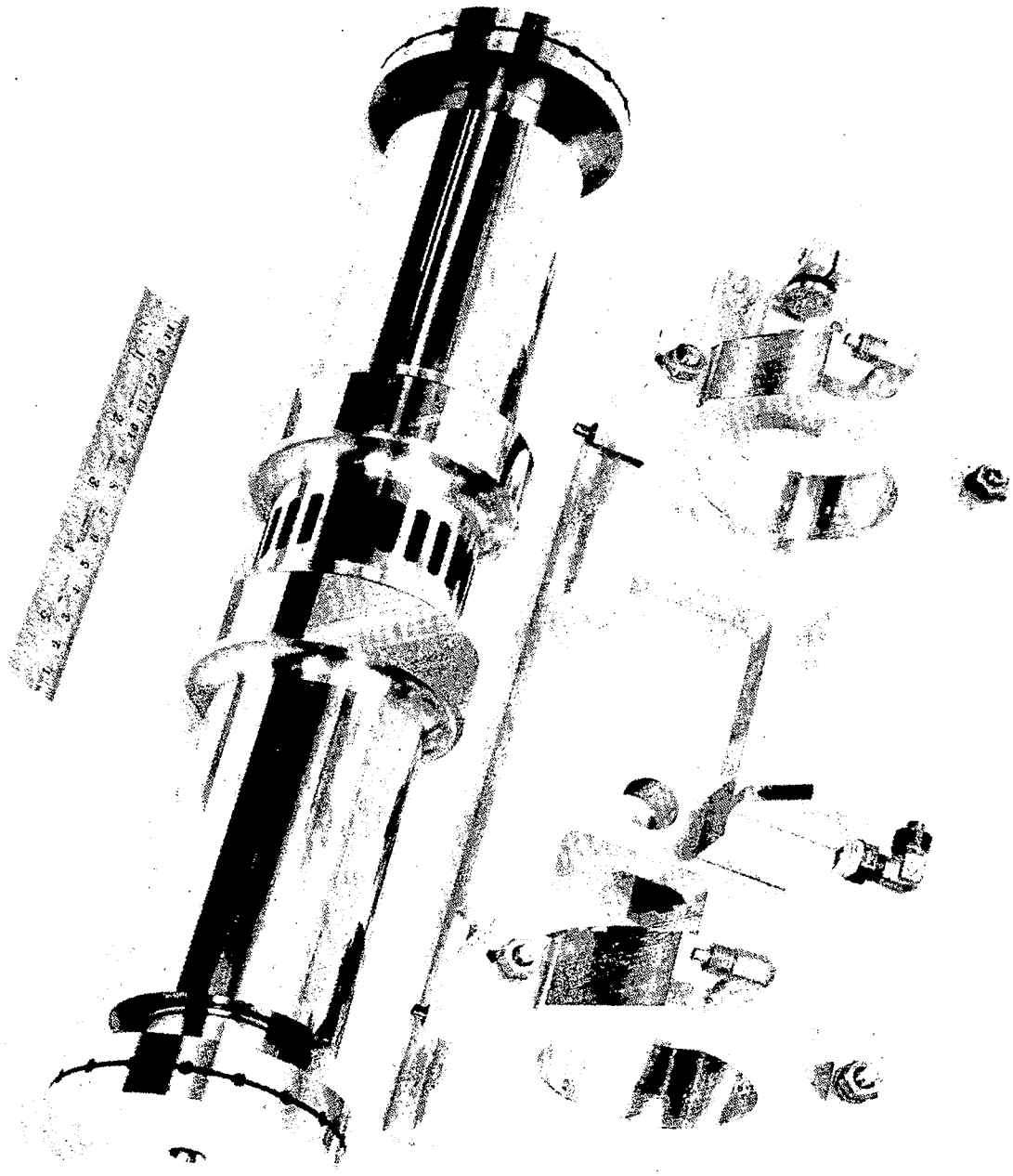

- ixture

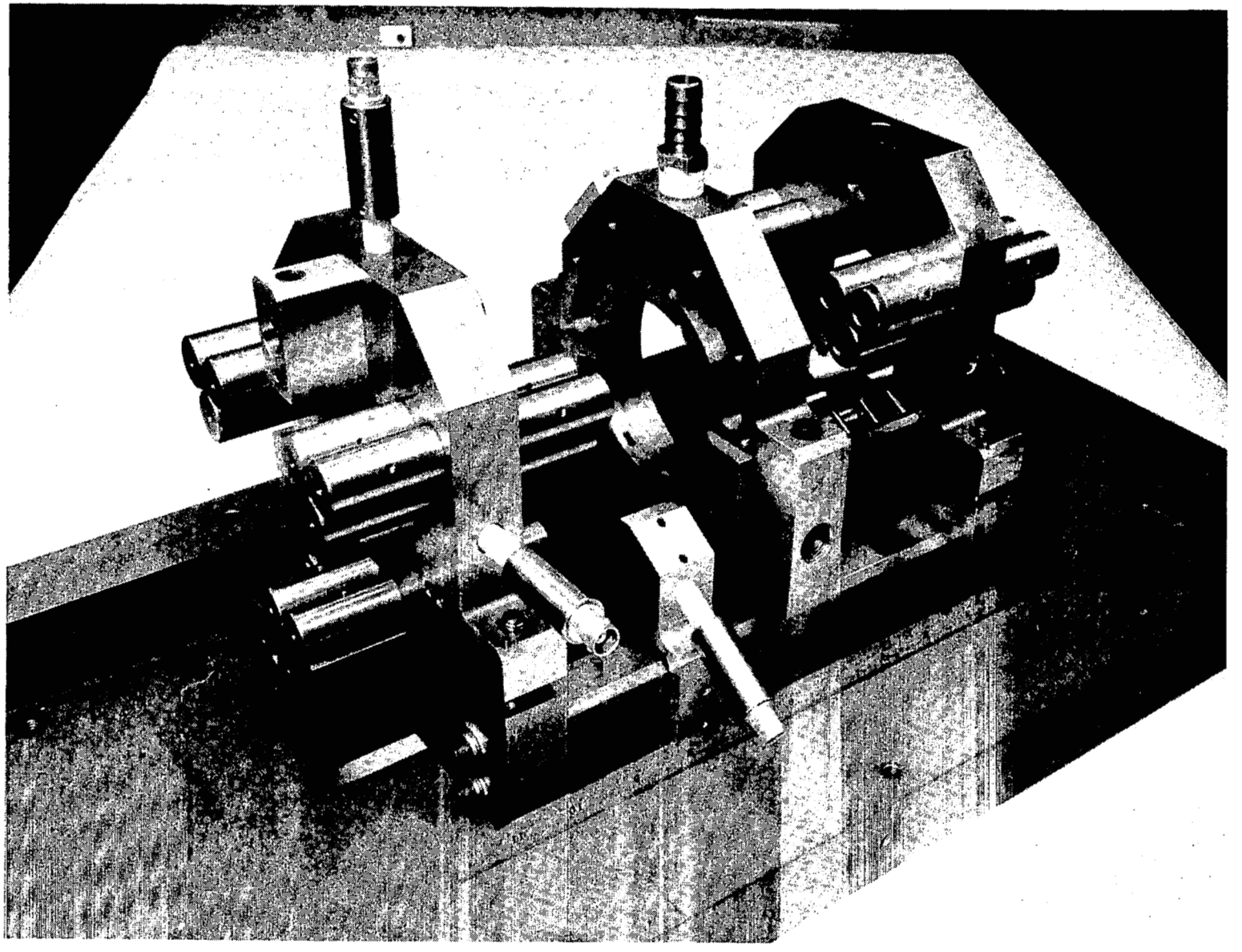

Fig. 4 View of Foil-Bearing Support Assembly

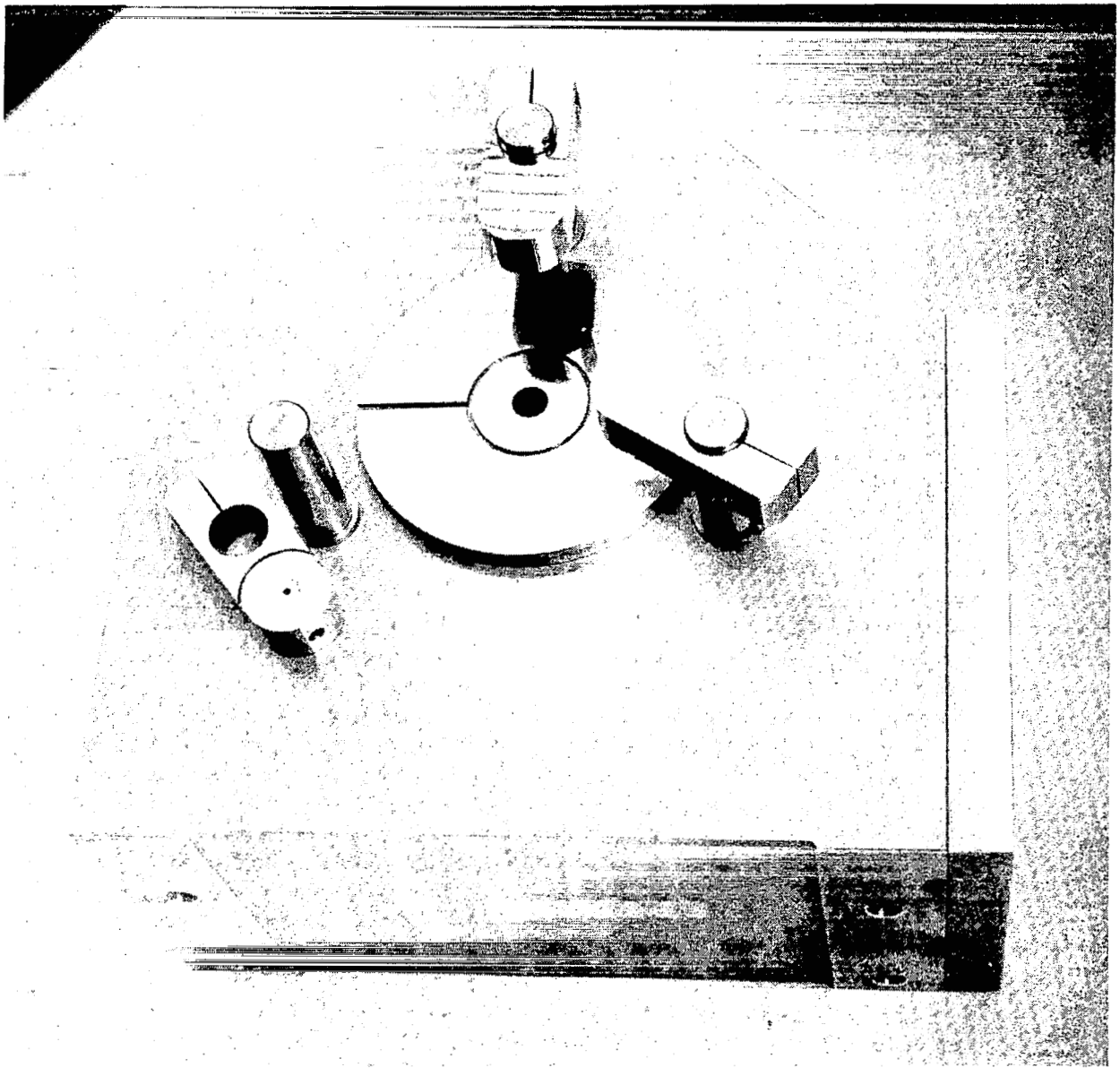

Fig. 5 View of Thrust Bearing Assembly

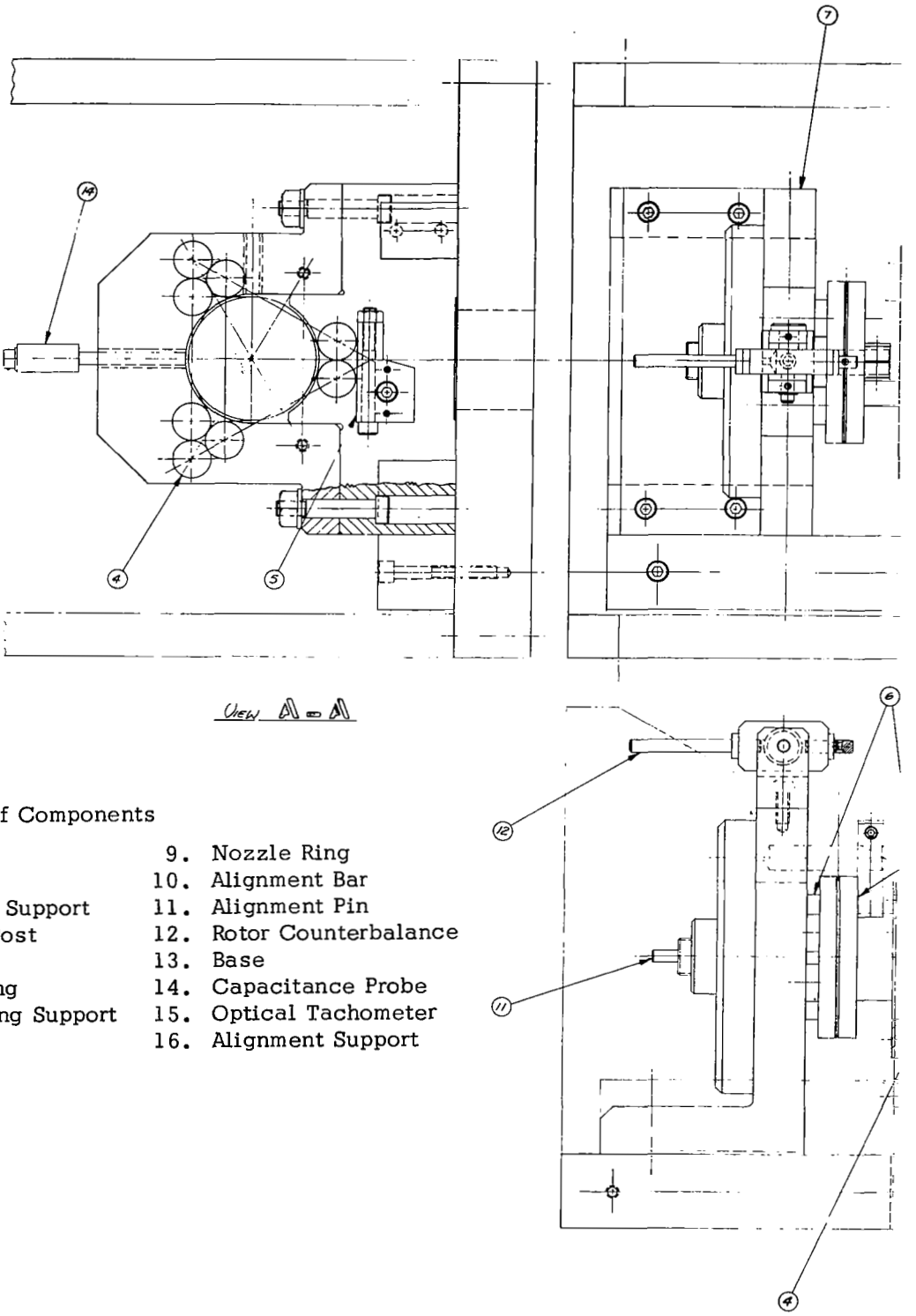

List of Components

1. Rotor
2. Foil Bearing
3. Foil-Bearing Support
4. Foil-Guide Post
5. Foil Lock
6. Thrust Bearing
7. Thrust-Bearing Support
8. Air Turbine
9. Nozzle Ring
10. Alignment Bar
11. Alignment Pin
12. Rotor Counterbalance
13. Base
14. Capacitance Probe
15. Optical Tachometer
16. Alignment Support

Fig. 6 Assembly Drawi

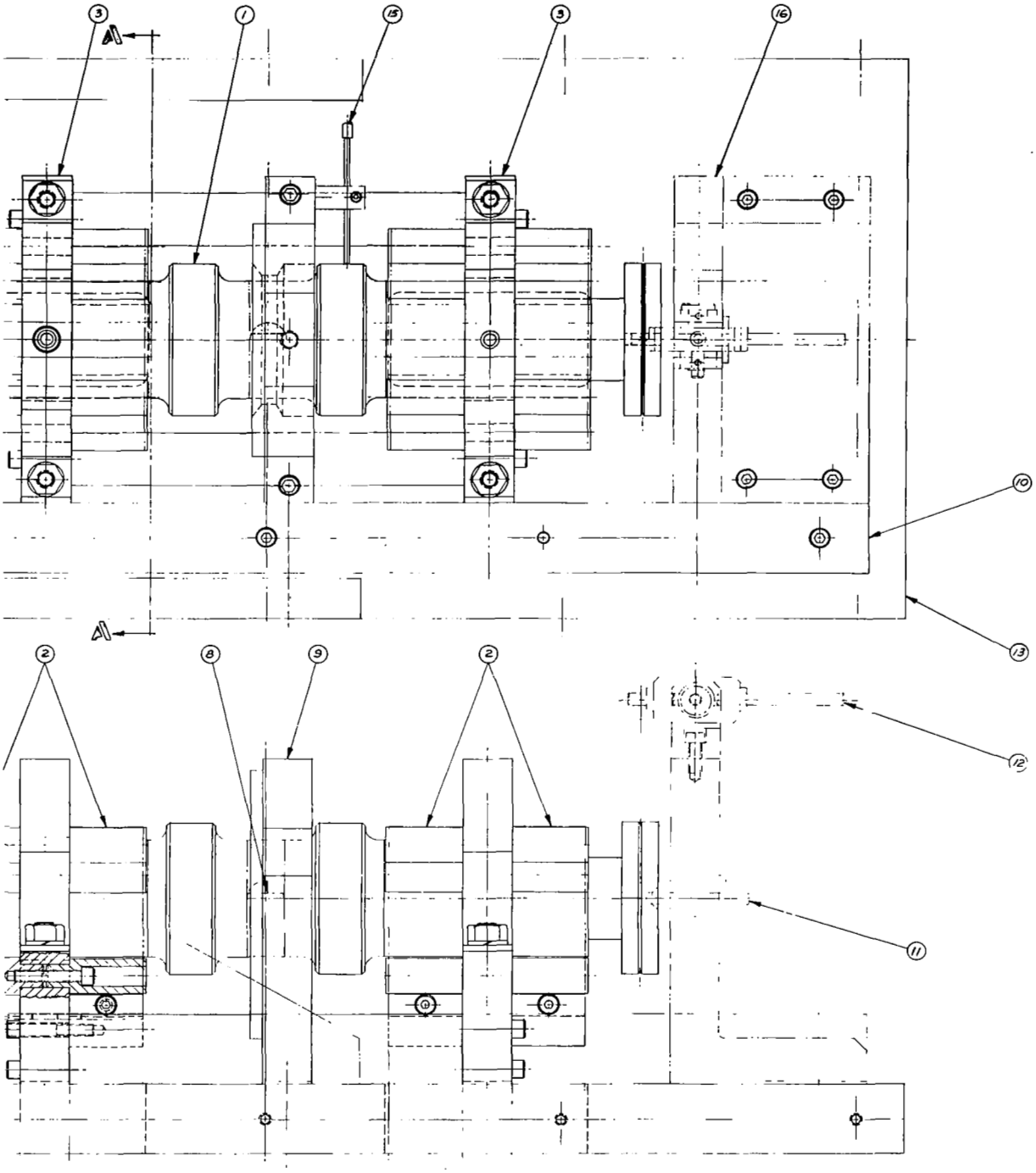

Experimental Apparatus

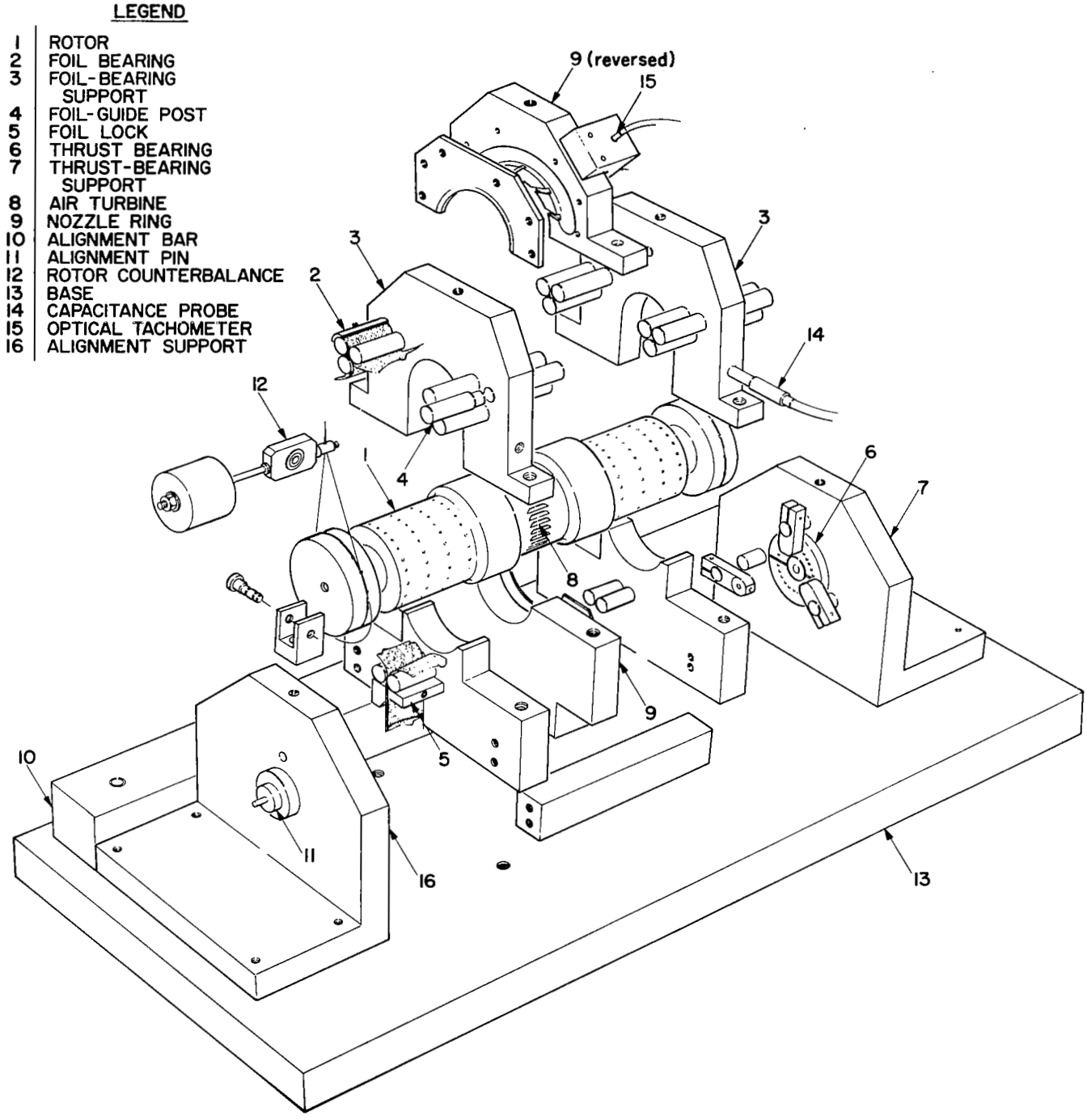

Fig. 7 Schematic Diagram of Experimental Apparatus

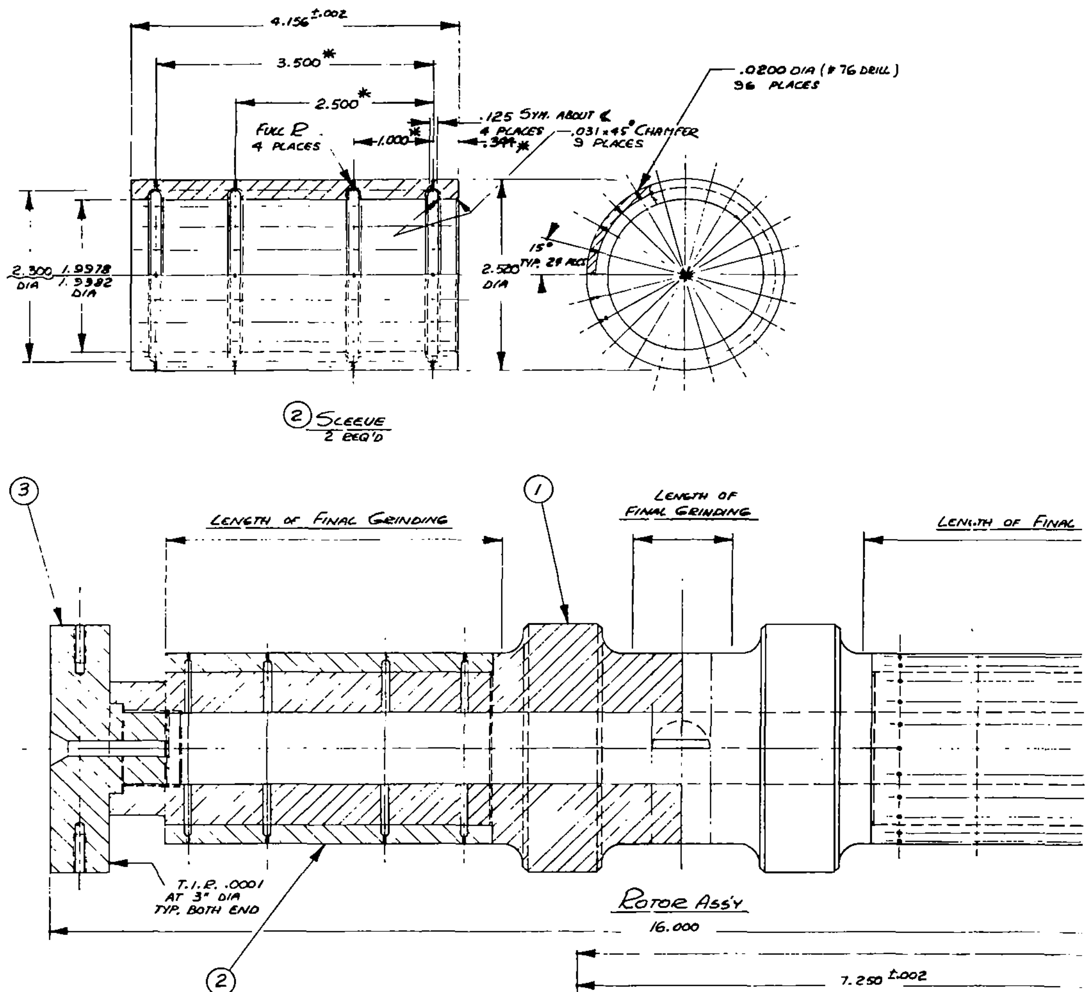

Note :

1. All Dimensions Marked with Asterisc (*) must have ±.001 Tolerances.

Instructions :

Parts	Annealing	Hardening	Stress Relieving	Shrink Fits and Assy	Remarks
Sleeves	Heat to 1550 – 1600°F, Soak and cool very slowly in furnace	Heat to 1850 – 1950°F and quench in oil (Gives approx. Rc-60). Do not exceed 1950°F	Soak for 2 hours at 300 – 350°F and cool slowly in furnace.	Heat sleeves to 775°F (do not exceed 800°F) and shrink on rotor body (Gives approx. Rc-58). Parts must be assly clean, no particles, scale, burrs or oil.	
Rotor Body					1.2506/1.2502 dia for end discs loc. Carbide tool finished after hardening of rotor
End Discs					

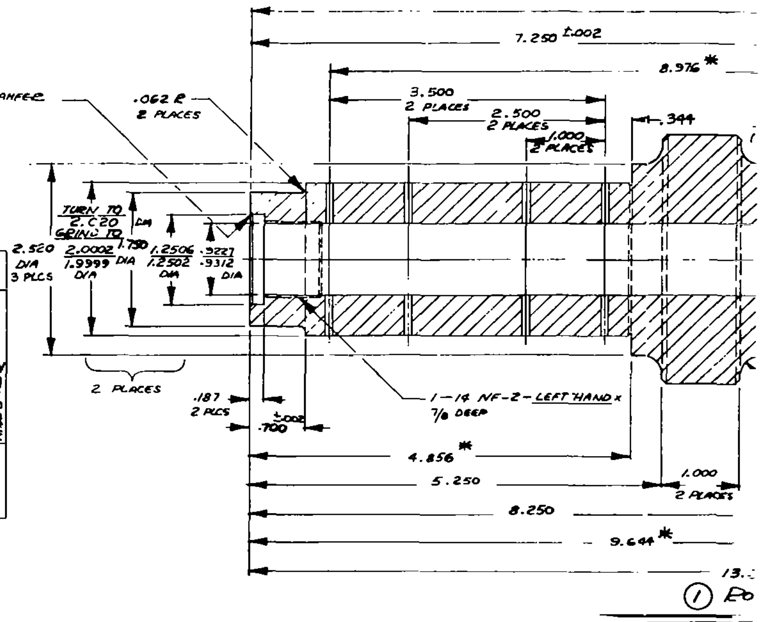

Fig. 8 Assembl

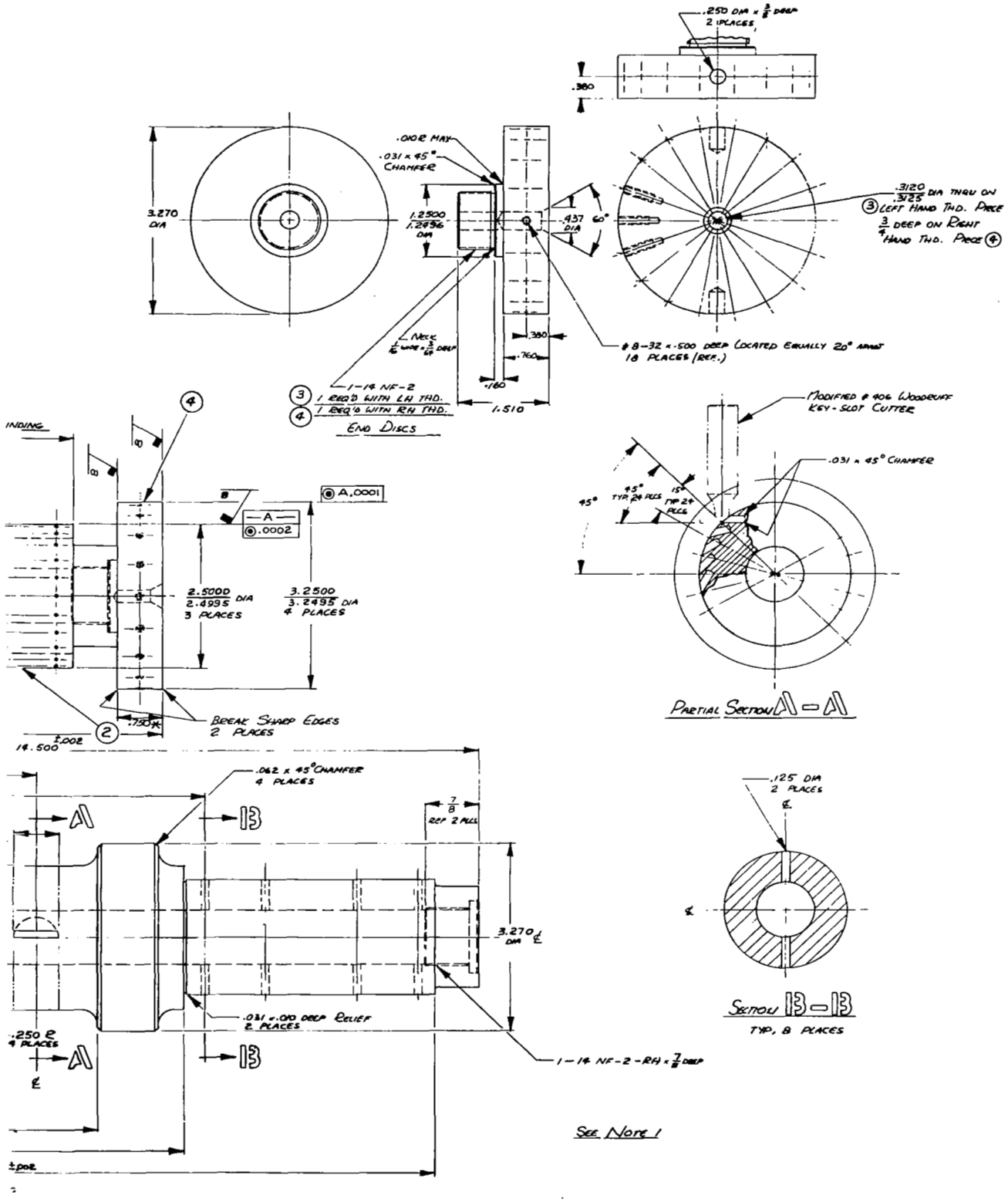

Drawing of Rotor

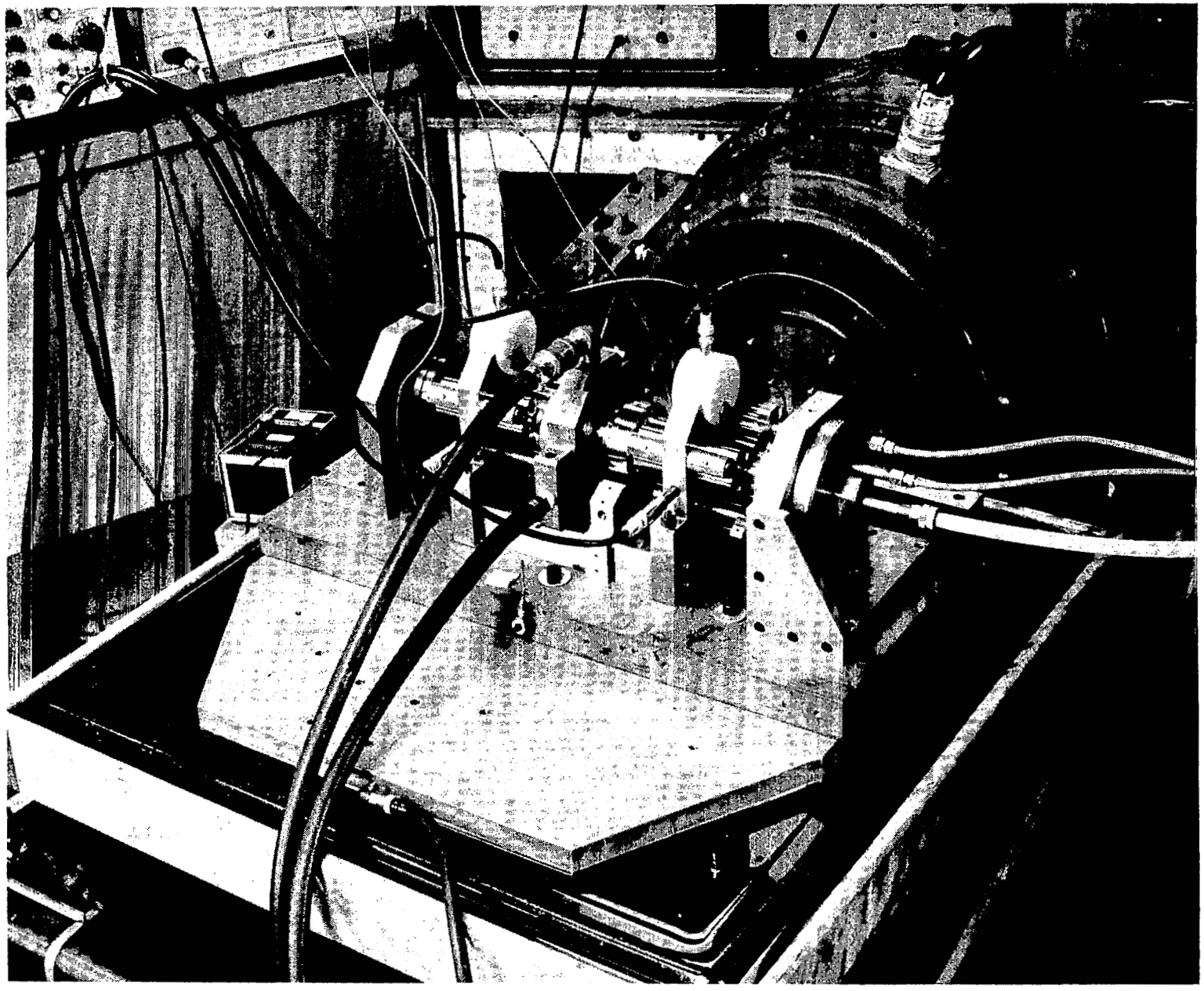

Fig. 9 View of Experimental Apparatus and Vibrator

3.0 INSTRUMENTATION

The orbital motion of the rotor was monitored by means of orthogonal capacitance probes, in the midplanes of two tandem foil bearings, spaced 9 inches apart. Provision was made for measurement of foil displacement at the midpoints of the 60 degree regions of wrap and also for the axial movement of the rotor.

The instruments used were Wayne-Kerr DM 100 Displacement Meters and the probes were calibrated by means of precision gauge blocks and an accurately ground cylinder of diameter equal to that of the journal. The gap width at the midpoints of several regions of wrap could be obtained directly by connecting the outputs of two parallel probes, one monitoring the displacement of the foil and the other that of the journal, to the terminals of a differential amplifier.

It is estimated that the amplitudes of motion of the rotor, based on the average sensitivity-scales appended to various oscillograms, involve maximum possible errors the order of 5%. This estimate includes variations of sensitivity between individual probes and the variation in sensitivity due to nonlinearity of probe outputs at relatively large probe offsets. The corresponding accuracy of scales in oscillograms of gap width is estimated to be within 10%. The frequency response of the displacement meters, inclusive of output filters, was flat to at least 2.5 kc and quite adequate in the range of experimental speeds of rotation and frequencies of excitation.

The speed of rotation was measured by means of an optical probe and an MTI KD-38 Fotonic Sensor, using a Hewlett-Packard

Model 523B Electronic Counter. Above 100 RPS, the speed could be measured and maintained with an accuracy better than 1%.

A digital-to-analog converter, integral with a Hewlett-Packard Model 560A Digital Recorder, was used in conjunction with a Model 523B Electronic Counter to obtain a d.c. signal proportional to the rotor speed.* This signal, applied to the horizontal plates of an oscilloscope, permitted direct photographic recording of the rotor amplitude-response and of foil clearance as functions of the rotational speed. It is estimated that the accuracy with which the rotational speed can be determined in the oscillograms of scans of the rotor amplitude-response and of the gap width is of the order 15 RPS, the error being due mainly to slow drift of the converter output. The recorder furnished automatically printed data of the variation of the rotational speed during coastdown, from which frictional losses could be calculated.

The vibrator (MB, Model C-10 Exciter) was capable of transmitting a force of 1200 lb within a frequency range 5 - 3000 CPS. Maximum displacement amplitudes of 0.5 inches and velocities of 70 in/sec could be realized. The accelerometers were Endevco, crystal type, used in conjunction with Glemite amplifiers, having a flat response 5 cycles to 35 kc. Since high frequency, low amplitude components of excitation, such as multiples of the rotational speed related to the number of nozzles, orifices, or turbine buckets, and other spurious high frequency disturbances could be sensed by the accelerometers, the amplified outputs of the latter were passed through SKL variable bandwidth filters to eliminate frequency components higher than 1500 CPS. This arrangement permitted proper control of motion of the vibrator by the in-line accelerometer and in a nearly sinusoidal vibration input to the rotor-support assembly, except at a number of isolated structural and foil-rotor resonances. A view of the experimental apparatus mounted on the vibrator table is shown in Fig. 9.

*Speed manually controlled.

In the course of experiments under largely non-isothermal conditions, the temperature of foils was measured by means of chromel-alumel thermocouples, at 6 collinear positions along the journal axis (3 per foil). The junctions and adjacent lengths of 0.003 inch diameter wires were brought into contact with the foil surface and were attached under a microscope with small amounts of a silicone adhesive.

The foil and journal surface temperatures were also determined by means of sparingly applied amounts of heat-sensitive coatings, available in increments of 25°F.* When applied in small amounts on the foil surface in the vicinity of thermocouple junctions, the melting of these substances on the foils could be observed in the course of experiments. Comparisons could thus be made between a number of melting points (in the range 200°F to 500°F) and corresponding thermocouple readings. These comparisons indicated that the thermocouple readings were approximately 10% to 14% lower than the specified melting temperatures of coatings and that the difference increased with temperature.

The heat-sensitive coatings were also applied at specific locations, close to the extremities of the journal adjacent to the heater, so that the highest surface temperatures attained at these points could be determined within discrete intervals of 25°F.

*Tempilaq, specified accuracy of melting point 1%.

4.0 EXPERIMENTS

4.1 Rotation in the Horizontal Attitude and Response to Residual Imbalance

The first series of experiments was conducted with the rotor in the horizontal attitude. A preload tension T_o = 2.0 lb/in was applied to the 0.001 inch thick, 1.5 inch wide molybdenum foils. The foil-lift supply pressure was p_ℓ = 30 psig. Upon removal of counterbalance weights, the rotor displaced downward by approximately 0.002 inch, returning to a position approximately 0.0003 inch below the reference axis when the foil bearings were externally pressurized.

The bidirectional thrust bearing consisted, in this set of experiments, of three 0.75 inch diameter pressure pads on each side of the thrust plate. Each pad was fed by a 0.028 inch diameter orifice and had a shallow 0.25 inch diameter, 0.032 inch wide pressure equalization groove. A pad supply pressure of 50 psig was maintained and the total axial clearance was 0.004 inch (i.e., 0.002 inch per side). In the pressurized mode of operation, the minimum clearance was 0.0014 inch because of dissymmetry produced by the thrust of the foil-lift supply pressure acting on the face seal. The minimum clearance corresponded to the inboard side of the thrust bearing, in which the outer perimeter of the thrust pads coincided with the 3.25 inch diameter of the rotating end disc, which served as a runner.

The test procedure followed in obtaining frequency scans of rotor response to remanent imbalance was to increase the speed very gradually (typically 2 - 3 RPS/sec, especially in resonant bandwidth) and to accelerate in the pressurized mode to approximately 300 RPS.

Following rapid cutoff of the foil-lift air supply and transition to the self-acting mode of operation, the rotor was accelerated to 750 RPS. After a few minutes of high-speed operation, during which speeds of 50,000 RPM were attained on numerous occasions, the turbine air supply was discontinued and the rotor allowed to coast down, first in the self-acting mode to approximately 300 RPS, and thereafter in the pressurized mode.

Typical scans of response during acceleration and coastdown are presented in Figs. 10 and 11. It can be seen that resonances occur in the pressurized mode only and that maximum amplitudes occur in a narrow bandwidth, centered at approximately 140 RPS. The resonant orbits, corresponding to maximum x- and y-amplitudes in the monitoring planes A and B that straddle each pair of foils, are shown in Fig. 12 . The timebase displays in the same figure indicate that the motion was quasi-conical. The maximum amplitude at the midplane of bearing A was the order of 775 μinches. In passing through the resonant bandwidth, the synchronous orbits displayed a very pronounced modulation at a very sharply defined frequency. One observes 24 cycles per revolution, and this corresponds to both the number of turbine buckets and the number of foil-lift orifices in each circumferential row. Since, however, the modulation could also be observed during coastdown, with the turbine inactive and foil pressurization on, the phenomenon may be attributed to the impingement of orifice jets on the foils. If so, it would appear that the response to an overharmonic excitation can be magnified at synchronous resonance. The two largest orbits in Fig. 12 were recorded at rotational frequencies immediately before and after the speed at which the modulation was most pronounced. The undulations are still discernible on traces corresponding to $(x_A)_{max}$.

The variation of gap width with speed in the horizontal attitude, at one of the load-supporting foil segments, is illustrated in Fig. 13 . At low speeds and in the pressurized mode of operation, the gap width was

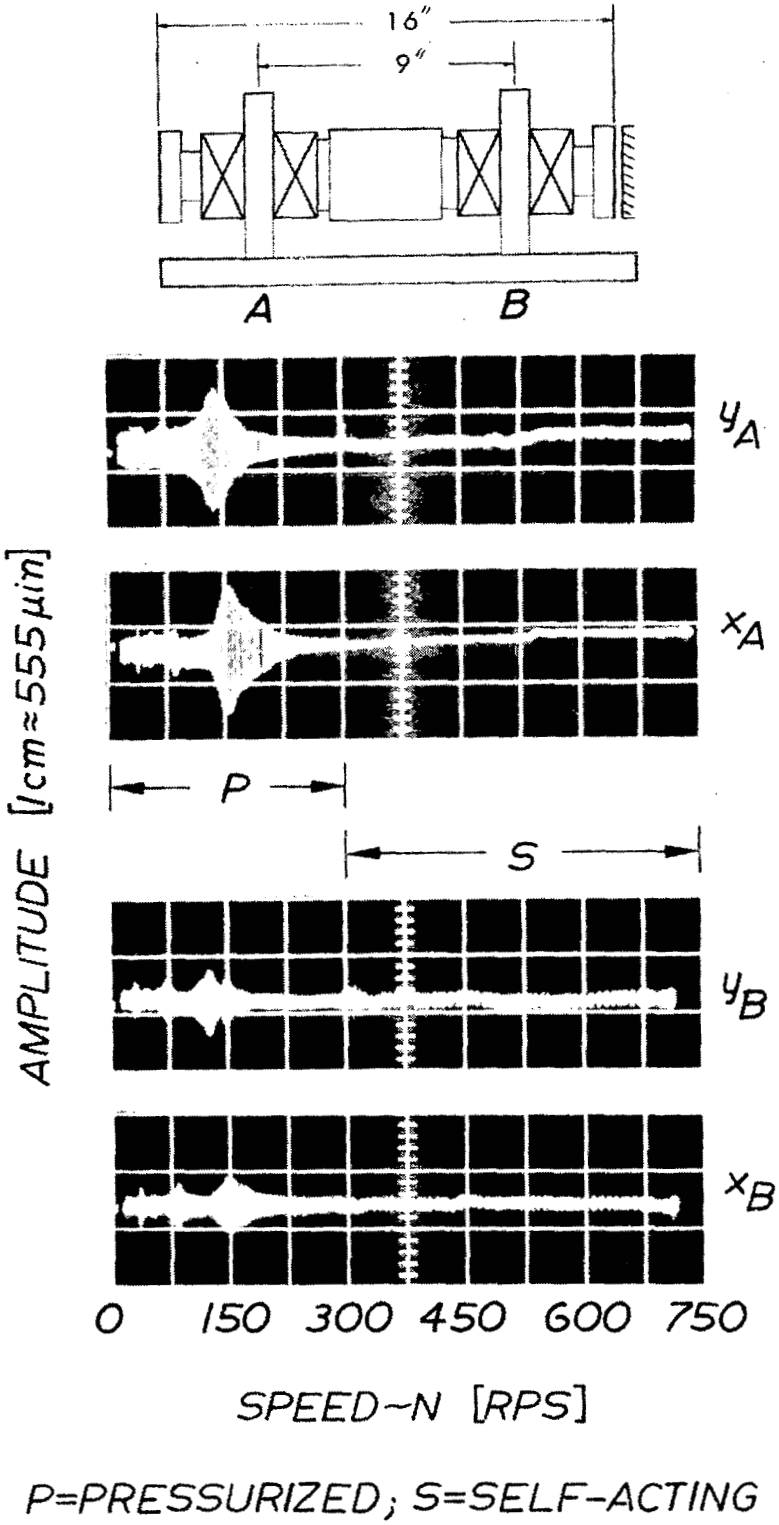

Fig. 10 Scan of Response to Remanent Imbalance in Horizontal Attitude (Increasing Speed)

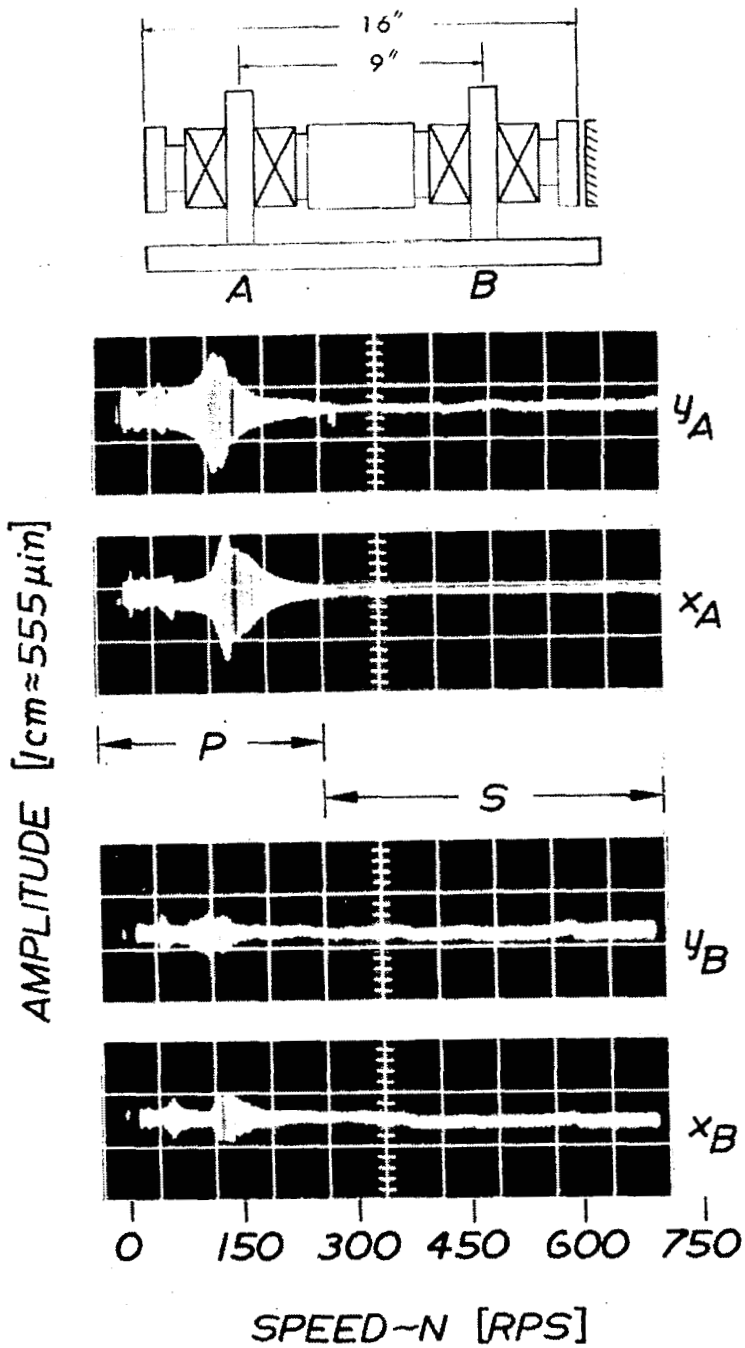

Fig. 11 Scan of Response to Remanent Imbalance in Horizontal Attitude (Decreasing Speed)

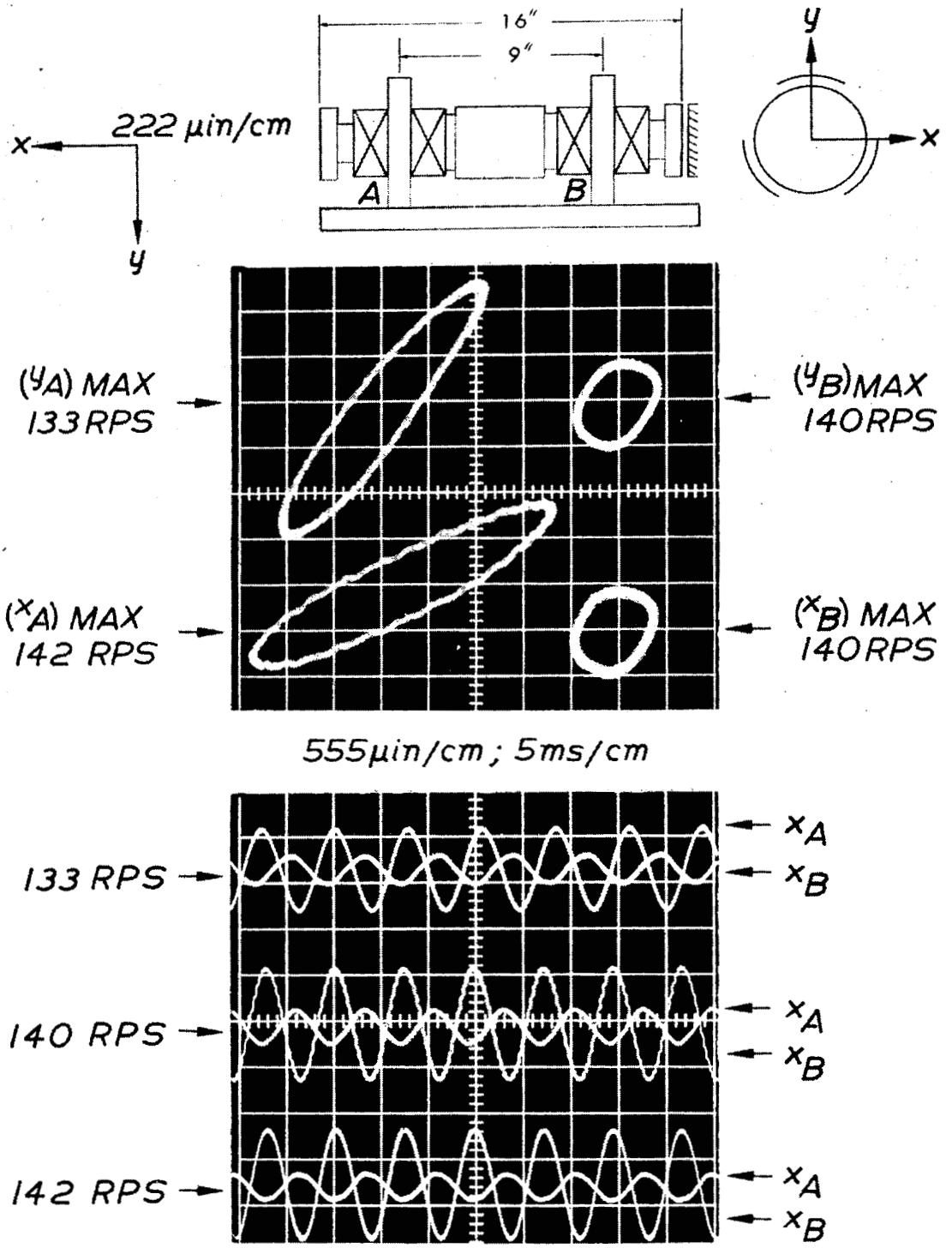

Fig. 12 Rotor Orbits at Major Resonances (Horizontal Attitude - Pressurized Foil Bearings)

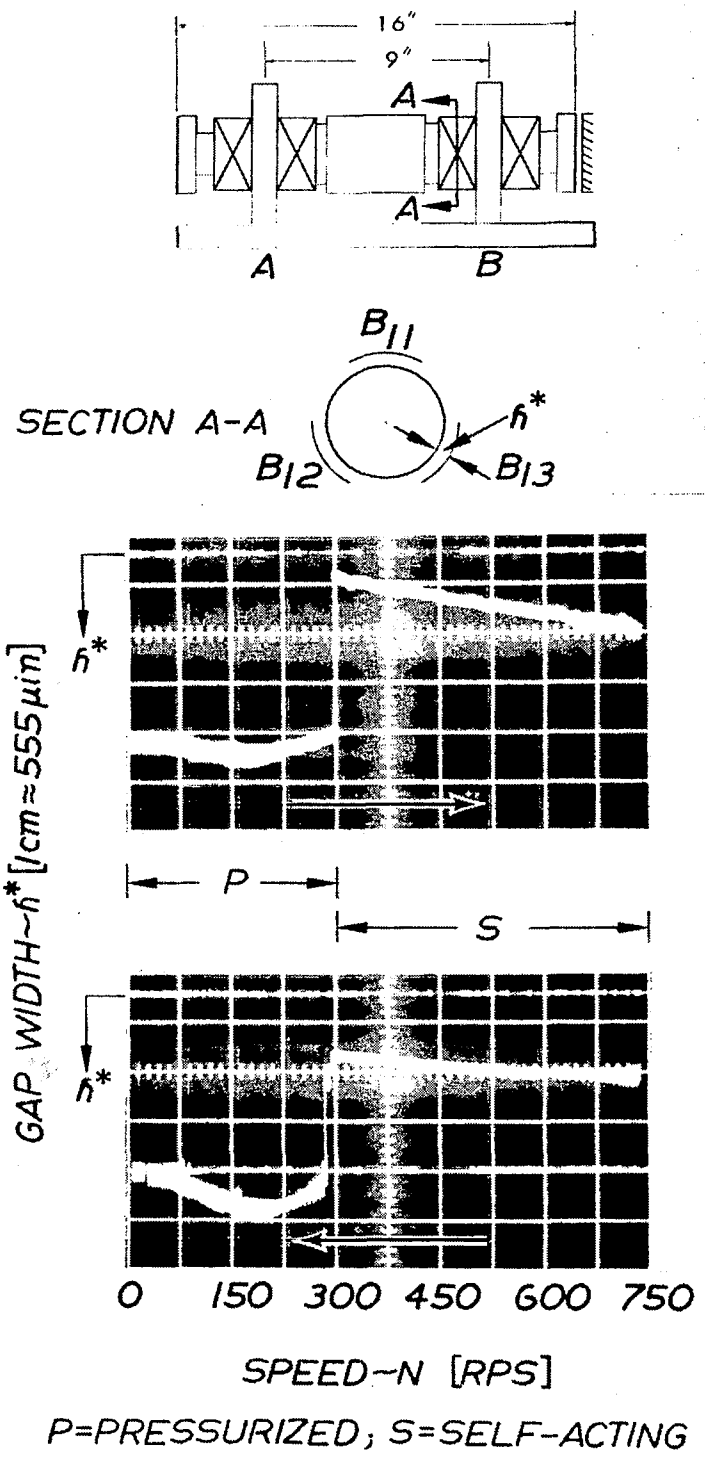

Fig. 13 Variation of Gap Width with Increasing and Decreasing Speed in Pressurized and Self-Acting Modes (Horizontal Attitude-Foil Sector B13)

the order of 0.002 inch, increasing noticeably due to squeeze film effects in the region of resonance. The decrease of gap width, following transition to the self-acting mode at approximately 300 RPS, is quite drastic. The clearance is diminished by nearly an order of magnitude to approximately 250 μinches, increasing to approximately 700 μinches at 600 RPS, and to 900 μinches at 750 RPS. On coastdown, the decrease of gap width with speed in the self-acting regime is moderated by additional slack, due possibly to thermal relaxation and following slippage of foil at the guides. During coastdown, just before re-pressurization, the clearance is approximately 700 μinches, and thus appreciably wider than following transition to the self-acting mode during acceleration of the rotor.

4.2 Response to Symmetric and Asymmetric Imbalance in the Horizontal Attitude

The remanent imbalance of the rotor, referred to the midplanes of the end discs (approximately 15 inches apart) was 350 μin-oz in each plane.* As noted in the preceding section, the maximum amplitude of response to remanent imbalance in the midplane of bearing A was approximately 775 μinches and occurred at a rotational speed of very nearly 140 RPS (Fig. 12).

Various amounts of symmetric and asymmetric imbalance were then introduced in the form of screws, in the midplanes of the end discs. The screws were of equal weight and the distances of their mass centers from the rotor axis were known within 2%

A comparison is made in Fig. 14 between maximum, or near-maximum, amplitudes at three levels of symmetric and asymmetric imbalance. The oscillograms of rotor orbits in the midplanes of bearing A

*The directions of remanent imbalances in each balancing plane could not be accurately determined. The magnitude of the imbalance vector can be determined with a much greater degree of certainty than its angular position.

and bearing B correspond to imbalances of 1,510 μin-oz, 6,050 μin-oz and 31,400 μin-oz in each plane. These levels correspond respectively to 4.4, 17.4 and 90.0 times the amount of remanent imbalance. The orbits in Fig. 14 were recorded in the pressurized mode at 140 RPS (resonance), and in the self-acting mode at 600 RPS (rated speed).

It can be seen that the maximum amplitudes* associated with highest level of symmetric and asymmetric imbalance were the order of 0.0013 inch to 0.0015 inch. At 600 RPS, in the self-acting mode of operation, the rotor amplitudes in the bearing midplanes remained below 250 μinches at the highest level of imbalance.

It is instructive to note at this point the difference between the gap width in a foil bearing and the clearance of a rigid-surface bearing. In the latter case, a 3 mil diameter orbit could hardly be accommodated within the clearance circle of a representative gas bearing. In the case of the foil bearing, both foil and journal can displace, without diminishing the clearance to dangerously small proportion. Should contact occur briefly, the distribution of load over the effective area of wrap of a flexible and conforming foil results in far less destruction than the concentrated loading due to impact and rubbing in a rigid-surface bearing.

During the first run in the vertical attitude, the experimenters inadvertantly omitted to remove the screws corresponding to the highest level of asymmetric imbalance and were consequently puzzled by relatively large orbits. The screws were removed and the experiments were not repeated in the vertical attitude, since the effect of imbalance in the presence of gravity load, in the horizontal attitude, represents a more adverse condition.

---

*To be interpreted as one-half of the maximum orbit dimension.

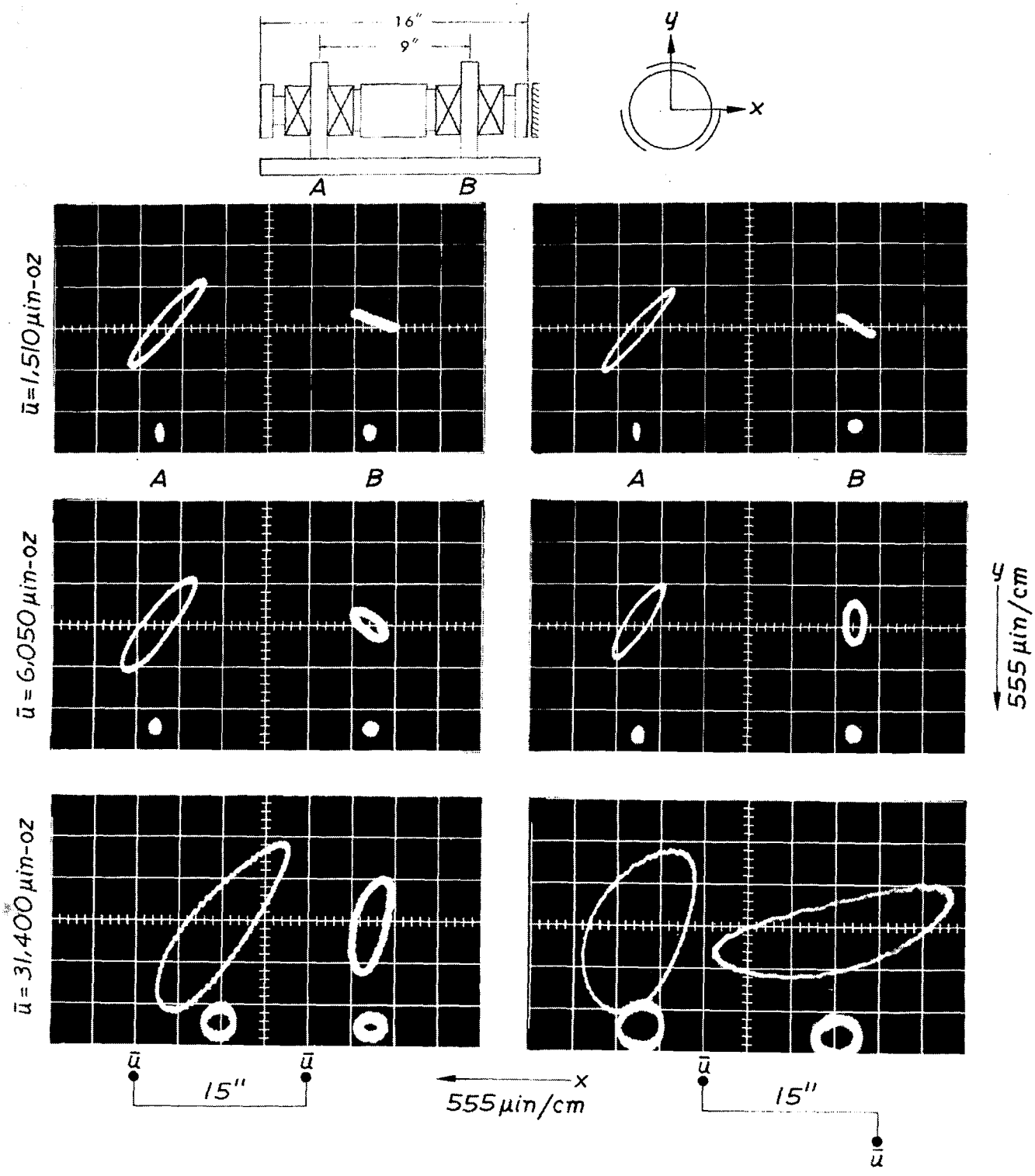

Fig. 14 Comparison of Orbits in Horizontal Attitude at Various Levels of Rotating Imbalance (Upper Orbits at 8400 RPM ~ Resonant Bandwidth) (Lower Orbits at 36, 000 RPM ~ Rated Speed)

4.3 Rotation in the Vertical Attitude and Response to Residual Imbalance

It is well known that conventional, fluid-film journal bearings, and gas bearings in particular, are plagued by the phenomenon of self-excited vibrations of rotors, frequently referred to in the literature as "half-frequency whirl," and more appropriately as "fractional-frequency whirl." This type of instability is particularly prone to occur with high-speed rotors operated in the concentric position, that is, in the absence of radial loading. The threshold speed of instability is very sensitive to the rotor mass, an increase of the latter having a very unstabilizing effect.

In the course of an experimental study of foil bearings, which preceded the present investigation [5, 6], no whirl instability was encountered with 1.0 lb and 2.4 lb rotors in either the horizontal or vertical attitudes and at speeds of 60,000 RPM. Results of the present investigation showed the operation of a 20.9 lb rotor* to be stable in both the vertical and horizontal attitudes at speeds up to 50,000 RPM, wherein the speed limit was dictated by the strength of interference fits of journal sleeves on the rotor, and not by imminent danger of instability.

The test conditions in the vertical attitude were identical with those described in the preceding sections, except that it was convenient to replace the three outboard pressure pads by a single, multi-orifice thrust plate, shown in Fig. 5. The 3 inch outside diameter, 1.1 inch inside diameter thrust plate contained 22 orifices (0.0145 inch diameter) located on a 2 inch diameter circle. The thrust plate was separated from the concentric face seal by venting grooves. The total axial clearance was 0.006 inch; the thrust plate supply pressure was 40 psig; the inboard pad supply pressure was 8 psig; and the foil-lift pressure 30 psig. In the pressurized mode of operation, with the thrust plate and face-seal pressures

*Based on unit projected bearing area, the masses of the three rotors referred to in the foregoing are in the ratio 1.0 : 2.4 : 2.8.

balancing the rotor weight and the added load of three inboard pads, the minimum clearance was 0.0013 inch (inboard side). In the self-acting mode, the minimum clearance was 0.0015 inch (outboard side). The foregoing data are furnished to show the limitations imposed by thrust bearing clearances on the permissible gyrations of the rotor in a quasi-conical mode. The diameters along which contact could occur on the rotating thrust member were 3.25 inches (edge of rotating disc on inboard side) and 3.0 inches (edge of thrust plate on outboard side).

The test procedure for runs in the vertical attitude was also identical with that described in the preceding section. Scans of response to remanent imbalance during slow acceleration and coastdown are presented in Figs. 15 and 16 and the differences between the respective oscilloscope traces appear to be minor. The maximum x and y amplitudes in the monitoring planes A and B occurred in the pressurized mode, in a narrow frequency bandwidth centered approximately at 140 RPS, which was nearly coincident with the resonant bandwidth observed in the horizontal attitude. The orbits corresponding to these maxima are shown in Fig. 17 , in conjunction with timebase displays of the x-probes. The latter are indicative of the motion of the rotor axis and the extent to which it is quasi-conical or quasi-cylindrical.*

Because of symmetry and approximately isoelastic properties of the foil-bearing supports, and because of the rotor mass distribution with respect to bearing location, the resonances corresponding to 4 degrees of freedom occur in a narrow frequency band and the peak amplitudes of all modes coalesce. These resonances are in the pressurized mode of operation

*The literature dealing with the motion of rotors in bearings abounds with references to "circular and elliptical" orbits and "cylindrical and conical" motions of the rotor axes. These simplified descriptions are convenient, but paths described by points on the rotor axis and surfaces traced by the axis itself are of far more complex geometry.

and it is evident that the resonant bandwidth of the self-acting mode lies well below the transition speed of 300 RPS.

It can be noted that scans of amplitudes of response in the low speed range display a series of rather well defined peaks, at definite speeds of rotation. While the orbits which characterize the maximum rotor excursions are synchronous, the orbits corresponding to the minor peaks are multi-looped, and the number of loops increases with decreasing speed. The relevant timebase displays show corresponding ultraharmonics superposed on the synchronous motion. This phenomenon of ultraharmonic resonances in the pressurized mode of operation was observed and has previously been described in references [5] and [6]. It was shown that the speed at which any ultraharmonic resonance occurred, when multiplied by the corresponding ultraharmonic number (ratio of orbital frequency to rotational frequency), was nearly equal to a speed of synchronous resonance. A series of orbits in the frequency bandwidth of the first ultraharmonic resonance is illustrated in Fig. 18 , together with corresponding timebase displays of the x-probes. Clearly, the rotor axis describes two revolutions for each revolution of the rotor about the axis. The reader will note that the average of the four speeds in Fig. 18 is approximately 67 RPS. Referring now to Fig. 17 , and taking the average of the four speeds, 138 RPS, as the speed of synchronous resonance, it will be noted that the latter occurs at very nearly twice the speed of the first ultraharmonic resonance.

Since most oscillograms were recorded with preamplifiers operated in the AC mode, they provide no information with respect to the overall displacement of the rotor axis with speed. This information is furnished in Fig. 19 , which contains oscillograms taken in the DC mode. It shows the displacement of the rotor axis with speed in the vertical attitude with respect to an initial reference position. The reference position was at zero speed, with pressurized foil bearings. When the

foils were returned to contact with the journals, the displacement of the rotor axis with respect to the reference line was in the order of 150 μinches. The displacement increased with speed in a direction subtending an angle of approximately 45^{o} with the x- and y-axes. The rate of displacement increased also with speed and the rotor axis displaced nearly parallel to itself for a maximum of approximately 600 μinches at 750 RPS. (See also [5, 6])

Three scans of the variation of gap width with speed were made in the vertical attitude. The first scan (Fig. 20) was made at the foil sector B_{13}, adjacent to the foil lock. This scan can be compared with the oscillogram presented in Fig. 13 , which corresponds to the same foil sector when radially loaded (horizontal attitude). In general, the gap widths appear to be of the same order of magnitude. During acceleration in the vertical attitude, the clearance immediately after transition to the self-acting mode was larger than in the horizontal attitude. Thereafter, the increase of gap width with speed in the horizontal attitude appears to have been greater than the increase in the vertical attitude. At 750 RPS, the gap widths in both attitudes were nearly equal.

All scans of gap width in the pressurized mode of operation display a relative maximum in the resonant frequency bandwidth, and this is attributed to an increase of the time-average pressure in the gap due to squeeze-film effects. In the pressurized mode of operation the measured gap widths at the foil sector B_{13}, in both the horizontal and vertical attitudes, were the order of 0.002 inch. At 300 RPS, in the self-acting mode, the clearances were the order 250 to 750 μinches, increasing to approximately 900 μinches at 750 RPS. It appears that gravity loading in the horizontal attitude is compensated largely by unloading of the upper foil sectors.

A comparison can also be made between the gap widths of two adjacent foil sectors, one on each side of the support plate A. The

results are presented in Figs. 21 and 22 and the oscillograms correspond to operation in the vertical (radially unloaded) attitude and refer to foil segments A_{21} and A_{11}. Both foil sectors were located opposite the foil locks. It appears that even in the vertical attitude appreciable differences existed between various foil segments with respect to the magnitude of gap width. At 600 RPS, for example, the gap widths of sectors A_{21} and A_{11} appear to vary by approximately 20%, but it must be emphasized that gap measurements were considered to be accurate to within 10% only. The reader is also alerted to the fact that the gap width decreases with tension and that relatively small extensions $\delta\ell$, comparable in magnitude with the gap width h^*, result in very appreciable increments of tension δT. † These differences and asymmetries are almost unavoidable in any realistic application. The encouraging fact is that the operational characteristics of the foil-bearing supported rotor seemed to be quite insensitive to these inherent nonuniformities, as evidenced by the successful operation of the simulator in both the vertical and horizontal attitudes.

Furthermore, it now appears that the foil bearing will fulfill expectations with respect to tolerance of distortions and variations of thermal expansions and other effects under largely non-isothermal operating conditions. Results of experiments at elevated temperatures and in the presence of appreciable temperature gradients are described in the following section.

Two coastdown curves from a speed of 750 RPS are plotted in Fig. 23. Although these plots correspond to operation in the vertical and in the horizontal attitudes, it can be seen that the curves are nearly congruent, indicating that frictional losses were nearly identical. The total frictional power loss at rated speed of 36,000 RPM, inclusive of windage,

† Note that, approximately, $h^* \sim T^{-2/3}$ and $\delta T/\delta\ell = Et/\ell \sim 10^4$.

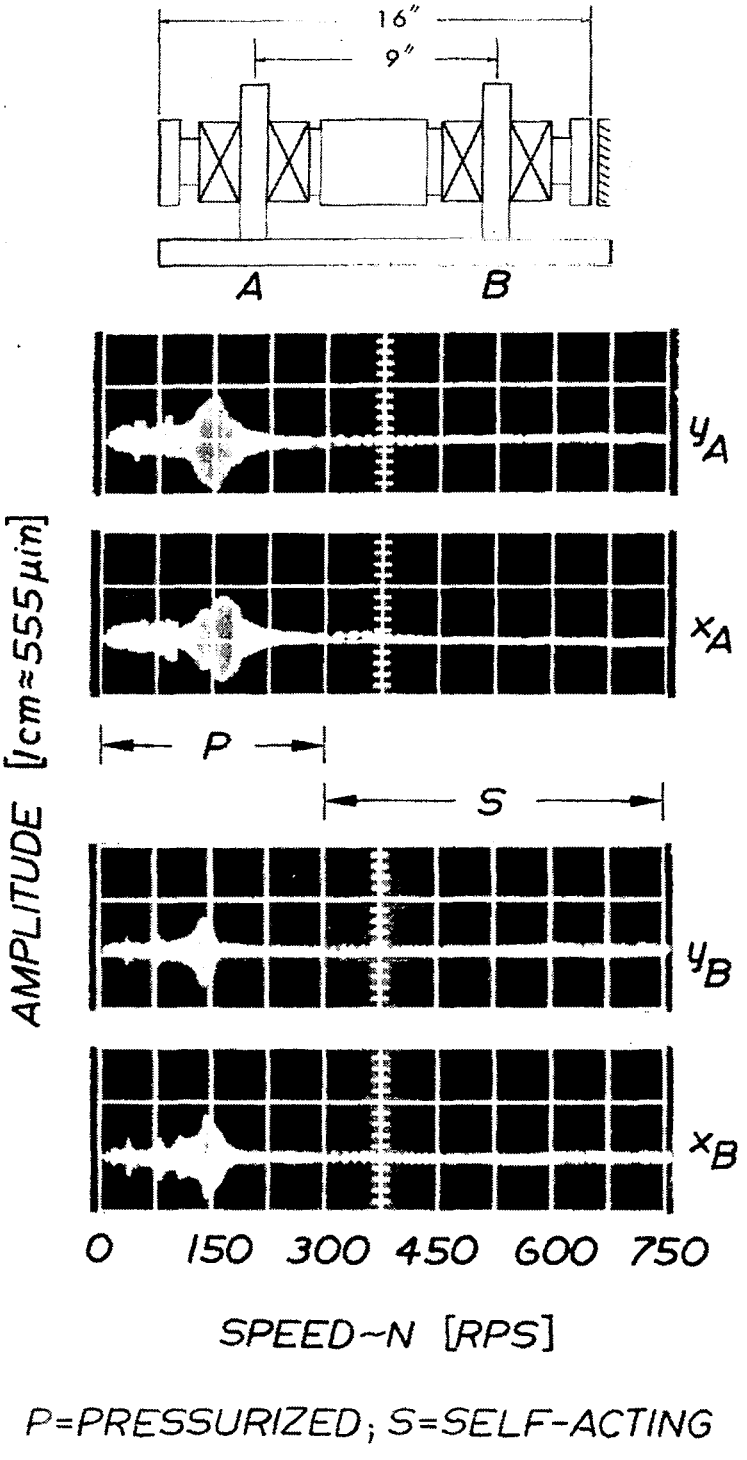

Fig. 15 Scan of Response to Remanent Imbalance in Vertical Attitude (Increasing Speed)

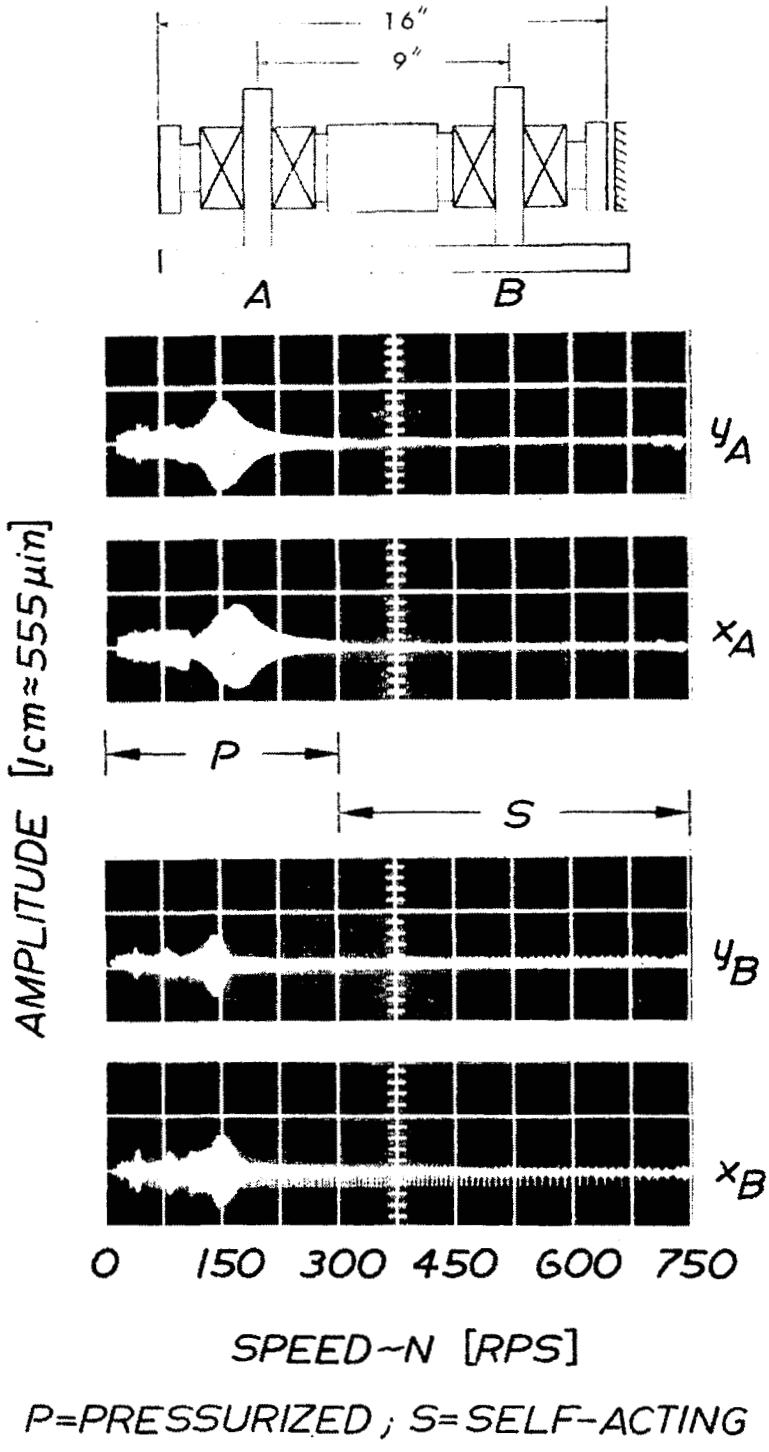

Fig. 16 Scan of Response to Remanent Imbalance in Vertical Attitude (Decreasing Speed)

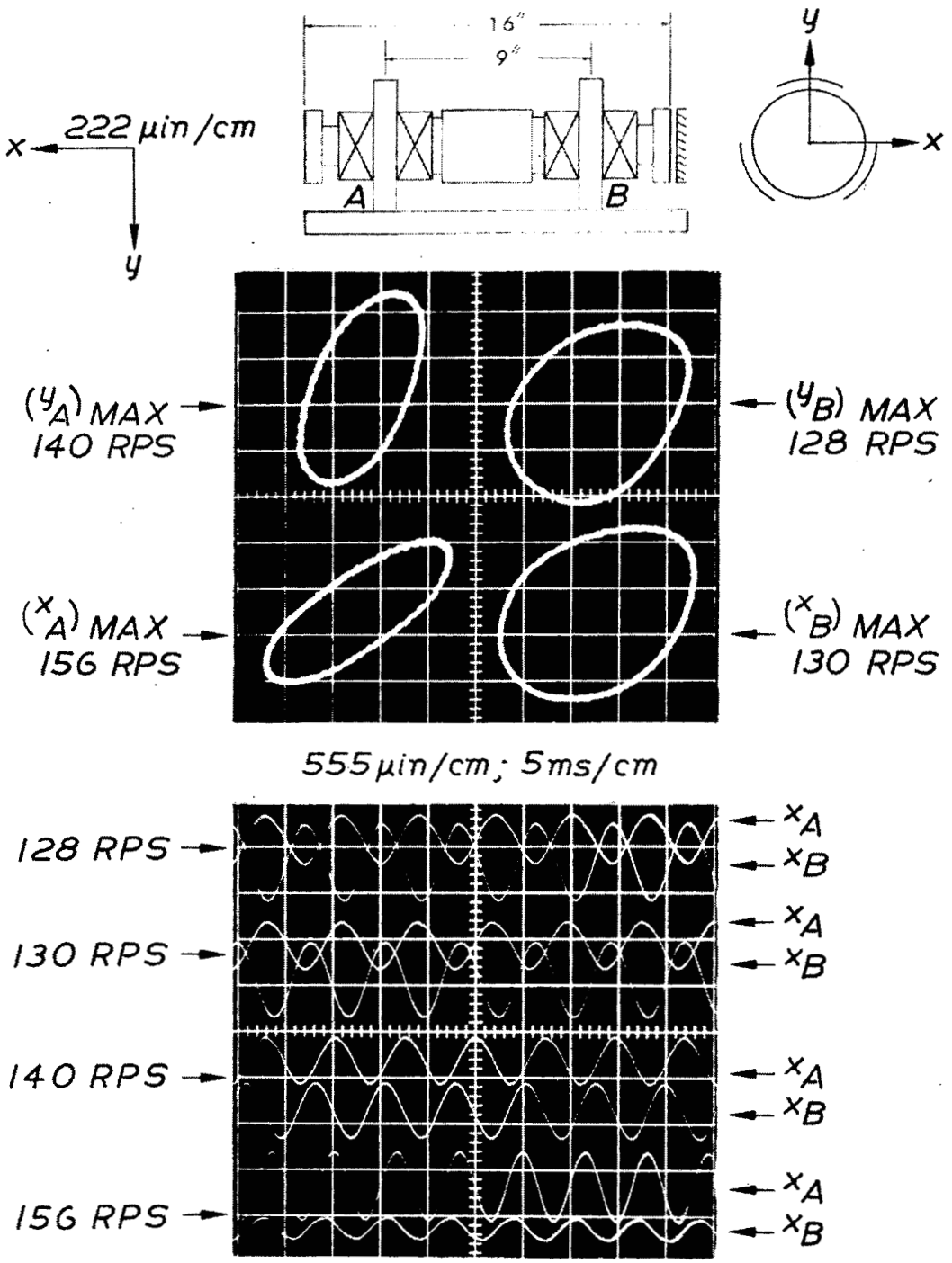

Fig. 17 Rotor Orbits at Major Resonances (Vertical Attitude - Pressurized Foil Bearings)

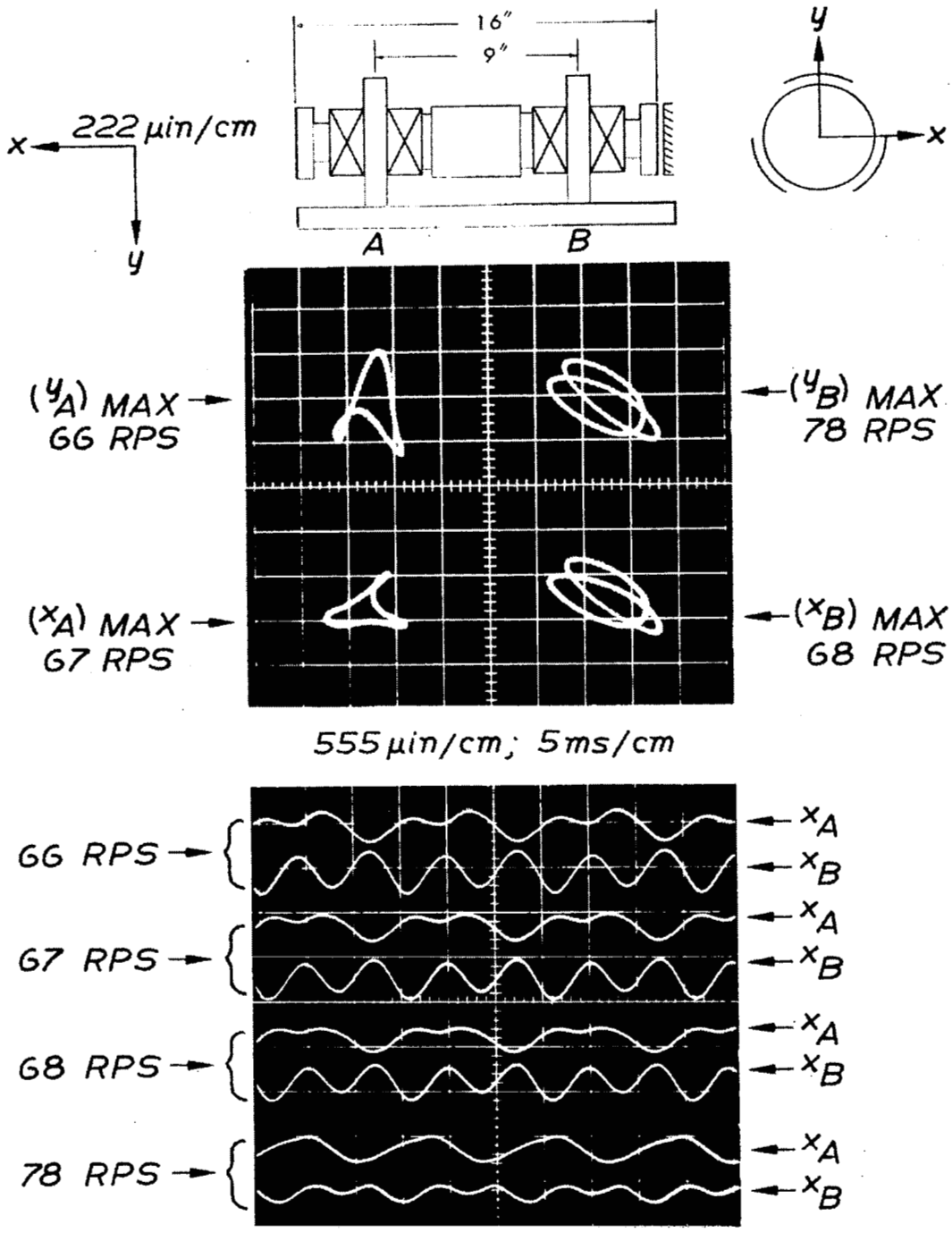

Fig. 18 Rotor Orbits at First Overharmonic Resonances
(Vertical Attitude - Pressurized Foil Bearings)

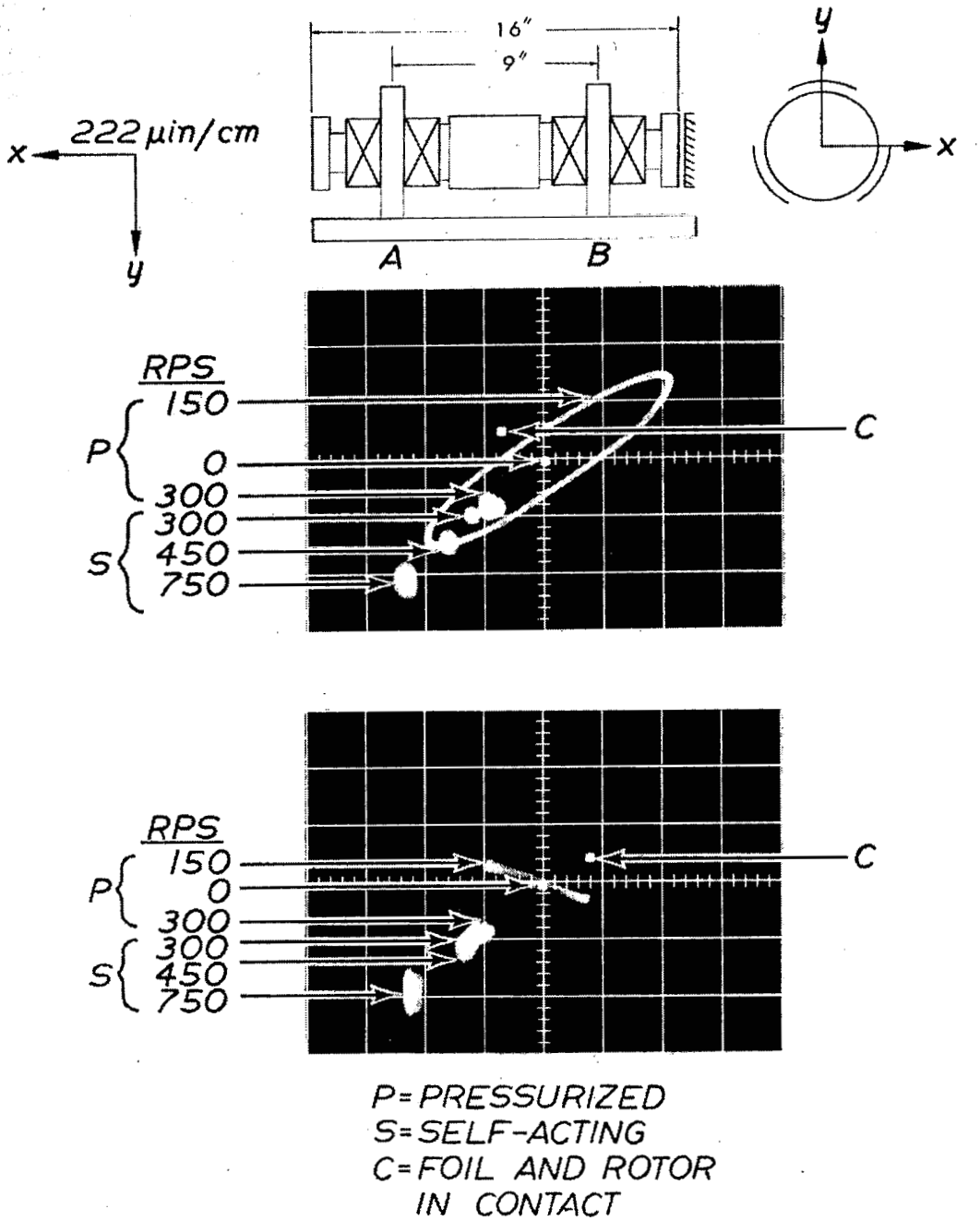

Fig. 19 Displacement of Rotor Axis with Speed
(Vertical Attitude)

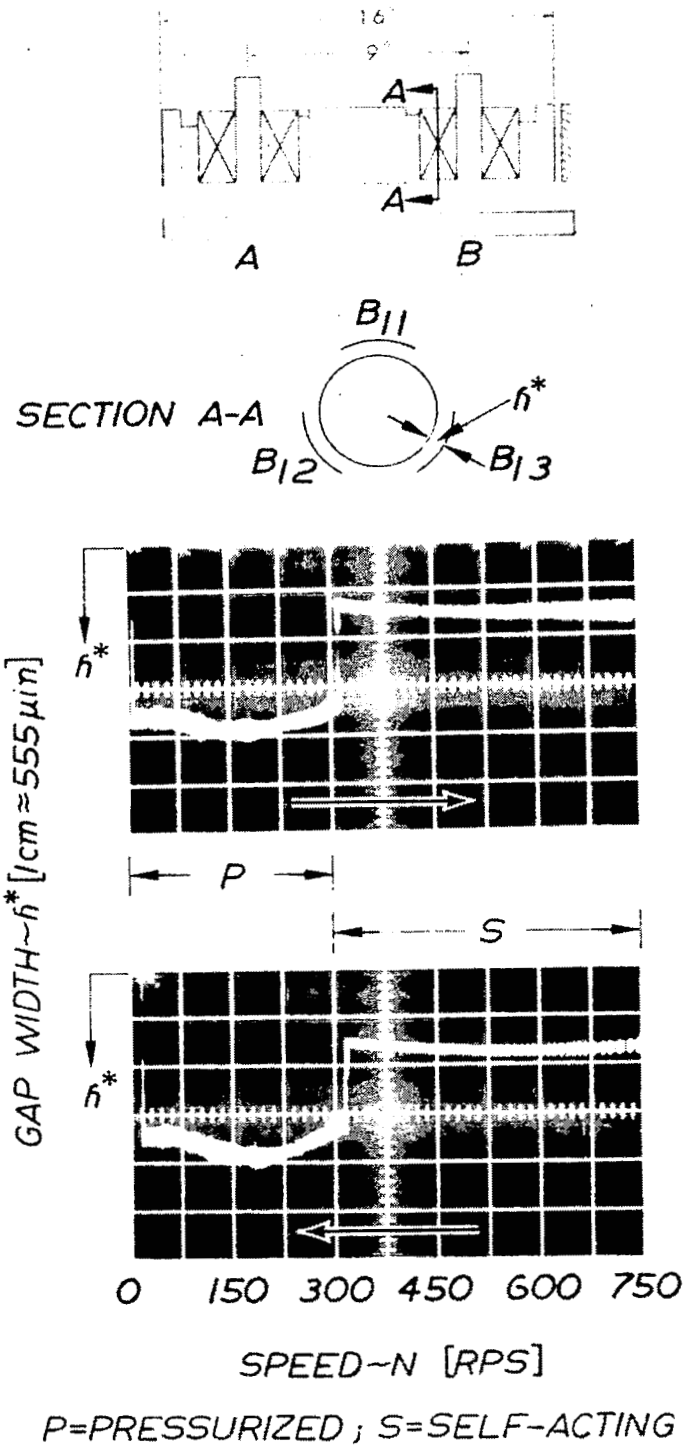

Fig. 20 Variations of Gap Width with Increasing and Decreasing Speed in Pressurized and Self-Acting Modes
(Vertical Attitude - Foil Sector B_{13})

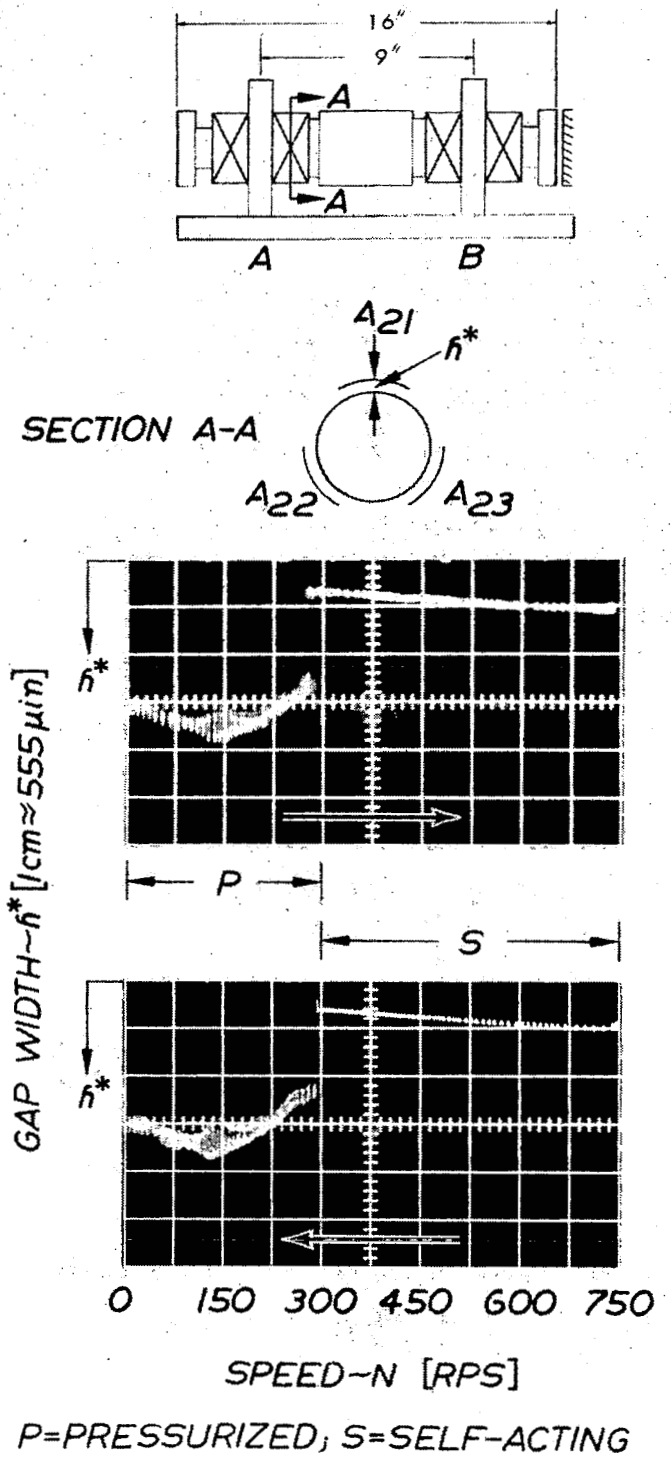

Fig. 21 Variation of Gap Width with Increasing and Decreasing Speed in Pressurized and Self-Acting Modes
(Vertical Attitude - Foil Sector A_{21})

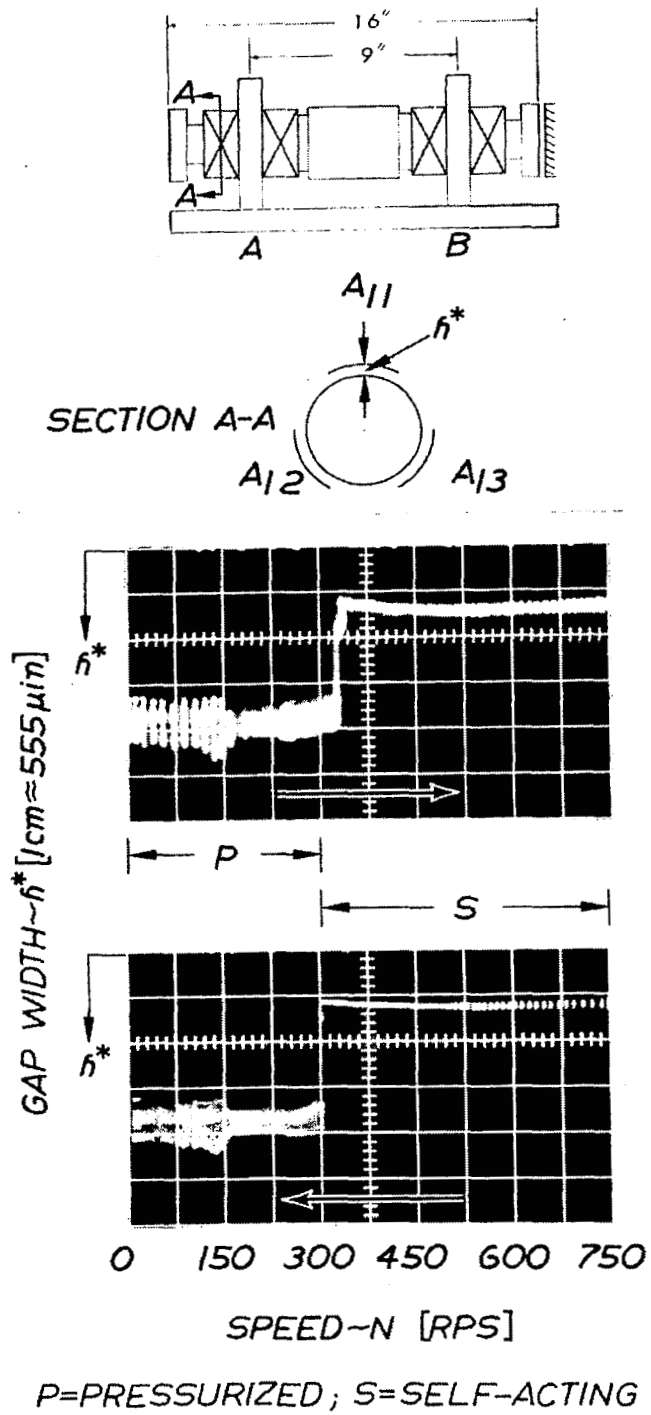

Fig. 22 Variation of Gap Width with Increasing and Decreasing Speed in Pressurized and Self-Acting Modes
(Vertical Attitude - Foil Section A_{11})

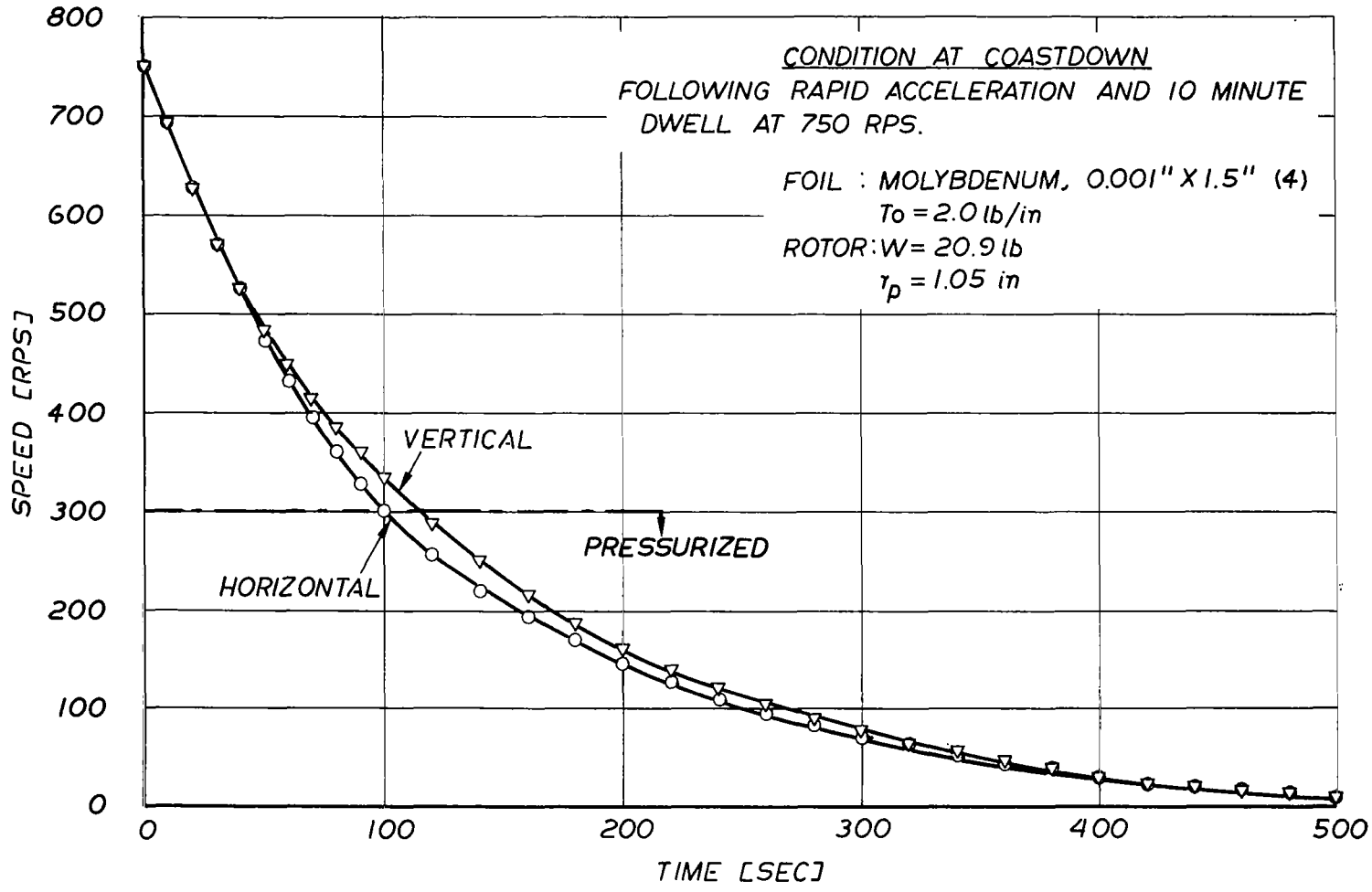

Fig. 23 Comparison of Coastdown Curves in Vertical and Horizontal Attitudes
(r_p = radius of gyration)

foil bearing and thrust bearing losses, was approximately 0.78 kw. An estimate, based on the assumption of simple Couette flow and an average gap width of 800 μinches, with air as a lubricant, shows the foil-bearing loss to be the order of 0.22 kw.

4.4 Effect of Heating and Temperature Gradients on the Performance of the Foil-Rotor System

In the case of gas bearings operated at elevated temperatures, serious difficulties are posed by thermal gradients and the accompanying thermal distortions. Not only is the performance of gas bearings extremely sensitive to clearance and the shape of the fluid film, but the mere existence of separation between journal and bearing surfaces may be threatened by differential expansion. The point is that gas-bearing clearances are relatively small, small in comparison with changes in journal and bearing diameters at elevated temperatures. The control of this difference in dimensions is always difficult. A gas bearing which provides a whirl-free and reliable rotor support in the absence of heating, and accommodates resonant amplitudes of motion within the nominal clearance circle, may pose a host of problems in a high-speed turbomachine operating at elevated temperatures.

The foil bearings, which have already proven their distortion-accommodating and superior wipe-wear characteristics in the absence of heating [5, 6], had not been previously operated in the presence of appreciable thermal gradients. To simulate the heat flow from the turbine to the adjacent journal and foil, a spirally wound heating element was placed at a distance approximately 0.1 inch opposite the rotating end-disc. Both heater and the turbine-simulating disc were placed in an insulating enclosure, consisting of a capped, cylindrical side-wall and a base with a 2-inch diameter opening.

The heater and thermocouple arrangement is illustrated in Fig. 24. The base of the heater was attached to the outboard set of foil

guides adjacent to the heating enclosure. The thermocouples numbered 1 through 6, six holders, and the location of junctions along the bisector of adjacent foil segments are clearly discernible in the view of Fig. 24. The thermocouples A and B were located within the heating enclosure. The shielded junction of thermocouple A was situated approximately 0.2 inch above the center of the heated disc and its temperature could be considered of the same order as that of the air in the heater-disc interspace. The junction of the fine-wire thermocouple B was located approximately 0.2 inch above the journal edge and approximately 0.003 to 0.005 inch from the short cylinder connecting the heated disc and the journal. Its maximum temperature was probably lower, but of the same order as the maximum surface temperature at the journal end. The output of thermocouple C was representative of the ambient air temperature in the vicinity of the test apparatus. The reader may note that the inboard (lower) foil in Fig. 24 was not swept directly by the cool turbine-air discharge, which was deflected around the inside radius of the rotor flange, just above the nozzle ring. The outboard (upper) foil was shielded from convective air currents by the foil support-plate and by a screen surrounding the foil and foil guides (placed between the heater base and the support plate and not shown in Fig. 24). The heater and thermocouple arrangement is also illustrated schematically in Fig. 25 and Fig. 28.

In addition to thermocouples, temperature-sensitive coatings were applied locally at various foil locations. The latter, though available at discrete intervals of 25° F only, had a specified accuracy of melting point of 1% and furnished useful means of estimating differences between foil and thermocouple temperatures. It appears that this difference, though relatively insignificant at temperatures the order of 200° F, showed the thermocouple readings to be lower by 10% to 14% at temperatures the order of 500° F. The foregoing should be taken into consideration in the interpretation of thermocouple data with respect to foil temperatures.

Thin layers of temperature-sensitive coatings were also applied close to the outer journal edge, and onto the journal surface just outside the foil edge adjacent to thermocouple No. 6. Parts of these coatings adhered with sufficient tenacity to withstand the centrifugal forces and finally melted, leaving tell-tale streaks and small traces of crystals as proof of melting at specific locations.

Histories of heating cycles in the vertical attitude were obtained at rated speed N = 36,000 RPM. In addition to thermocouple readings and observation of melting points of coatings on the foil surface, recorded also were the approximate heater power input and the turbine nozzle supply pressure required to maintain rated speed. The history of the first heating cycle, of approximately 2 hours' duration, is presented graphically in Fig. 25. The foils used in this experiment were 0.001 inch thick molybdenum (coefficient of thermal expansion 2.7×10^{-6} in/in/^{o}F - as compared with 5.6×10^{-6} in/in/^{o}F for AISI 440-C, the rotor material - and modulus of elasticity approximately 47×10^{6} psi).

After a 30 minute warm-up without heat input, the rate of power dissipation in the heater was increased rather rapidly. Because of thermal lag and delay in power-supply cutoff, the temperatures attained in the vicinity of the journal and foil edges adjacent to the heater exceeded greatly the intended magnitudes, reaching approximately 800^{o}F at the foil surface and, possibly, even higher temperature at corresponding points on the journal. Closure of the gap required increased power to drive the rotor, as reflected by the increase of supply pressure at the turbine nozzles from 51 psig to 68 psig. The rotor, nevertheless, continued to operate smoothly at 600 RPS and the orbital motion was negligibly small.

Since rising foil temperatures, despite first diminished and then discontinued heat input, indicated a very large reduction in gap width, and possibly some metal contact, the rotor was coasted down after

approximately 2 hours of operation (Fig. 25). The third coastdown curve in Fig. 26 indicates that deceleration was very rapid and that the usual increase in gap width, due to pressurization, may have been overshadowed by local contraction of the foil along rows of cooling orifice jets.

Despite rather excessive heating in the course of the first run, there were two rather surprising and encouraging aspects of the experiment. The first was that the rotor remained operational and that it has been possible to maintain high-speed rotation under such adverse thermal conditions. The second, and even more surprising experience, was that that the rotor, after a short period of cooling, could be restarted and did perform faultlessly throughout the entire experimental speed range. We anticipated also that foil and journal damage might be quite extensive. It now appears, as will be shown in the following section, that these fears were not justified.

The temperature profiles along bisectors of two adjacent foil-bearing segments recorded at various times in the course of the first run are shown graphically in Fig. 27. Disregarding the 125-minute curve as far too extreme for conditions to be anticipated in an actual turbomachine, we note that the minimum foil gradients of the 105-minute and 85-minute profiles are the order of 135°F/in and 125°F/in respectively.*

Prior to the second experimental run with heat input, the 0.001 inch thick molybdenum foil adjacent to the heater was replaced by an Inconel-600 foil of equal thickness. The objective of this change was to obtain a better matching of coefficients of thermal expansion to compensate for dimensional changes of rotor, foil and foil supports. (The coefficients of thermal expansion of metals involved in this case were

*The corresponding axial temperature gradients on the journal surface would be at least as steep, or steeper.

2.7, 5.6, 6.5 and 7.4 μin/in/^{o}F for molybdenum, AISI 440-C, AISI 416 and Inconel-600 respectively). Some relief was also to be expected as a result of lower extensional rigidity of Inconel-600, due to its lower elastic modulus. The duration of the run was approximately 8 hours, at rated speed N = 36,000 RPM.

The history of this heating cycle and corresponding foil-temperature profiles are illustrated graphically in Figs. 28 and 29. In this experimental run, successive increments of power input to the heater were smaller and spread over longer time periods. The rotor was first accelerated to rated speed and operated without heat input for 90 minutes, allowing the foils to reach equilibrium temperatures. It can be seen that the energy dissipated in shearing the air film produced a sensibly uniform temperature the order 180^{o} F along the shielded, outboard foil. The inboard foil, exposed to convective air currents, was cooler, with temperature dropping in the direction of the air turbine. The latter furnished an efficient heat sink in the midplane of the rotor.

The temperature attained by the outer edge of the journal was between 575^{o} and 600^{o} F. The maximum temperature attained at the other journal extremity, approximately 0.125 inch from the foil edge , was less than 125^{o}F. The maximum temperature of the foil adjacent to the heater was between 525^{o} and 550^{o}F, dropping by approximately 100^{o}F across the width of the foil. The corresponding differential across the inboard foil was also the order of 100^{o}F, from a maximum between 350^{o} and 325^{o}F. The foregoing values were established on the basis of melting points of temperature-sensitive coatings.

The highest bearing temperatures attained in the course of this run were approximately 30% lower than the maxima reached during the first run, but generally higher than values to be encountered in an actual machine. The supply pressure at the nozzles (Fig. 28) was increased from

51 to 57 psig only, rather than to the 68 psig level of the previous run, indicating appreciably lower frictional losses. The temperature profiles in Fig. 29 indicate operational foil gradients the order of 70° F/inch.

In the absence of availability of preheated foil-lift air, the rotor was allowed to cool at 600 RPS and was coasted down when temperatures approached equilibrium. A comparison of the coastdown curves is made in Fig. 30. The first curve corresponds to a condition in which both rotor and foil temperatures remained close to ambient. The second curve reflects a slight increase in friction when coasting down after near equilibrium temperatures were attained, following cutoff of external heat input. Figure 31 shows that differences in rotor response during coastdown from near equilibrium temperatures, prior to and following the 8-hour run, were minor. Note that replacement of one of the four molybdenum foils by an Inconel foil had no drastic effect on the rotor response. The ultraharmonic orifice-jet excitation (n = 24) is amplified at discrete speeds in the bandwidth of synchronous resonance and the effect is clearly discernible in the orbits of Fig. 31.

In the course of preliminaries to experiments at elevated temperatures, attempts were made to operate the rotor at high speeds and in the pressurized mode. The objective was to provide a relatively large and safe operating clearance during coastdown, without cooling at rated speed. Early pressurization would insure against excessive reduction of gap width at low speeds when coupled with an adverse combination of thermal expansions . (Indeed, with preheated gas readily available in a turbomachine, the full benefit of early pressurization could be realized without the conflicting effect of local cooling of the foil by orifice jets experienced during the first non-isothermal test.) The result of these preliminary experiments was very gratifying, because stable operation in the pressurized mode and in the vertical attitude was achieved up to 36,000 RPM. The

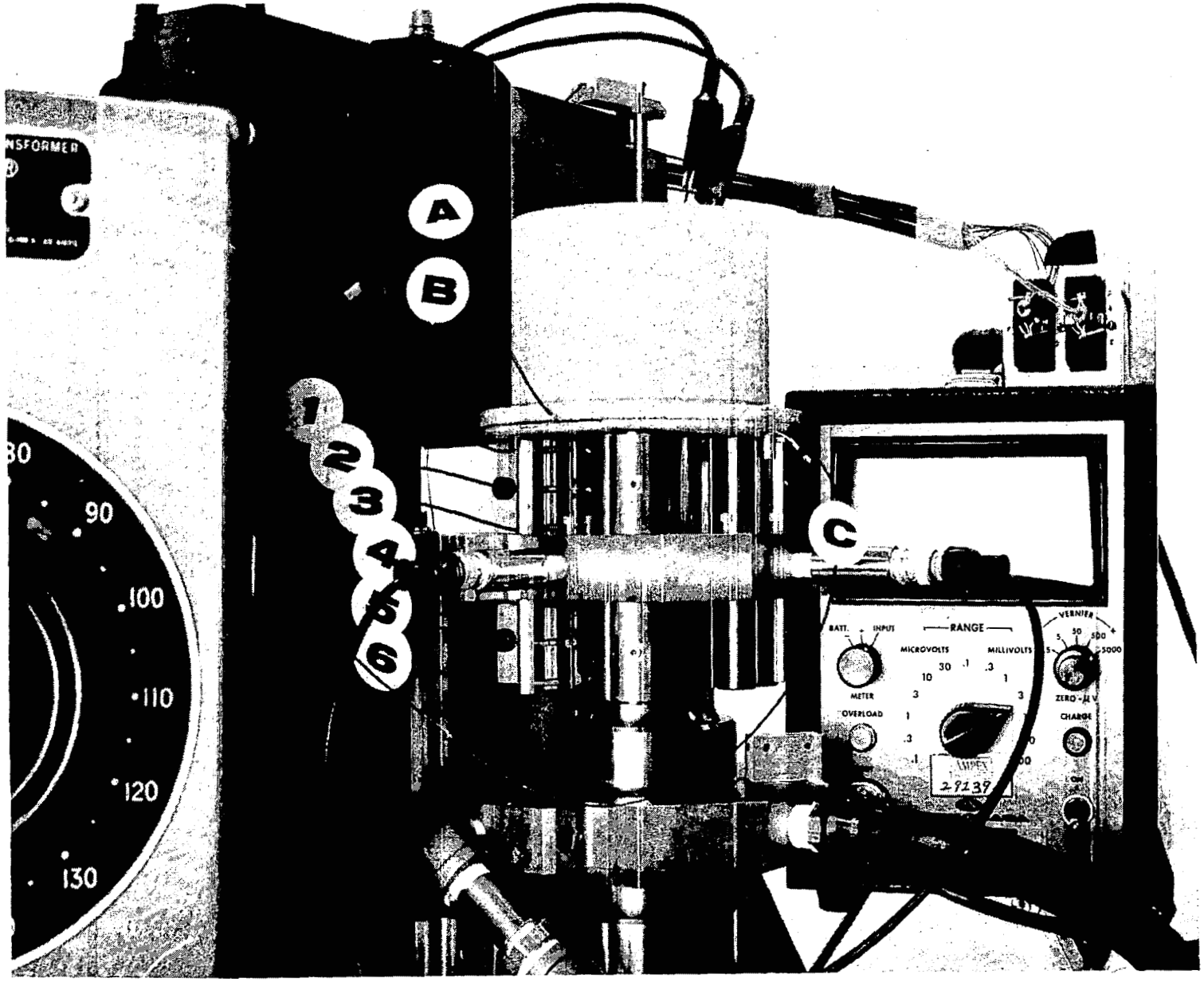

Fig. 24 View of Heater, Foil Bearing and Thermocouple Arrangement

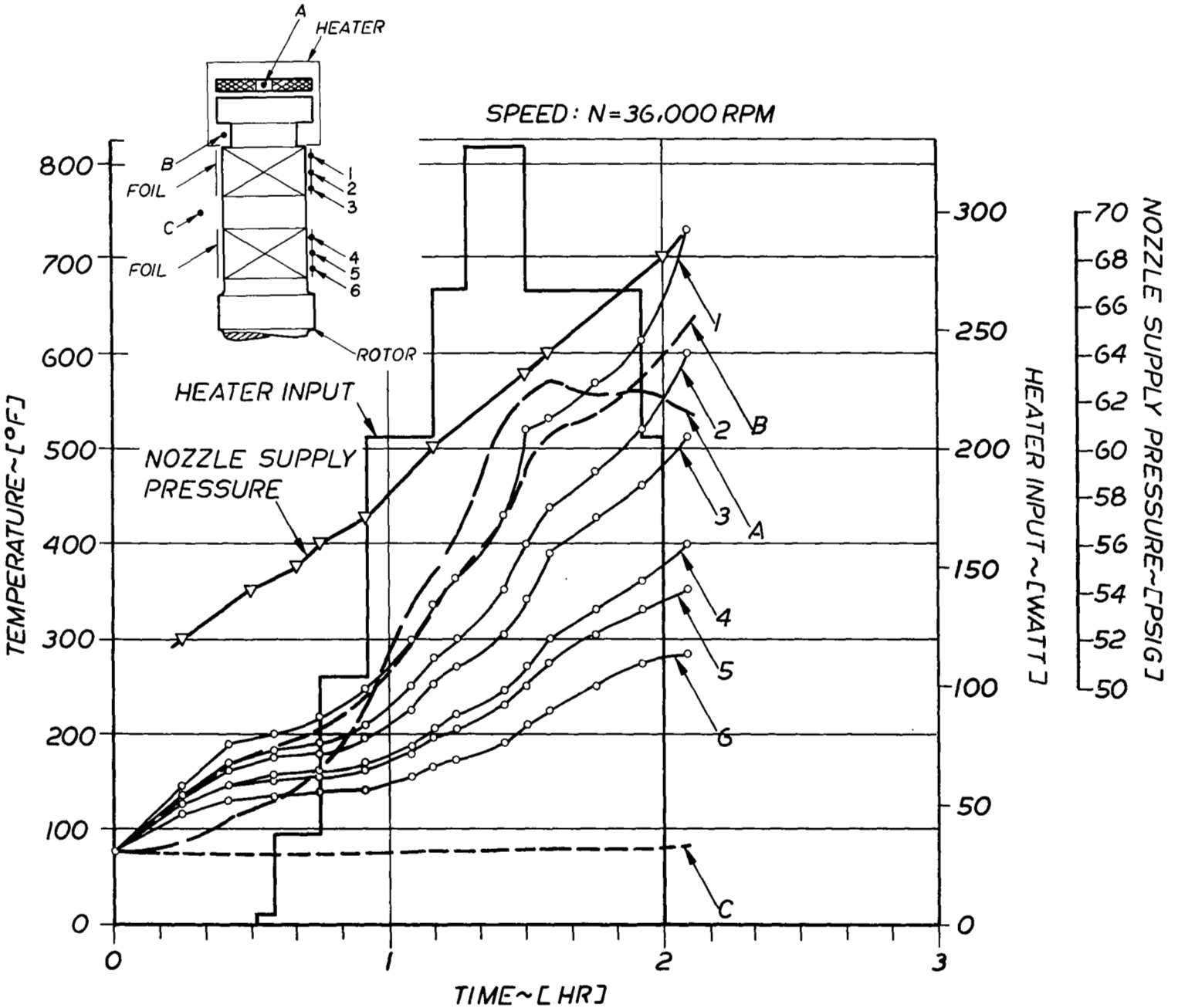

Fig. 25 Temperature Record of Heating Cycle
(Rotor Vertical - Molybdenum Foils

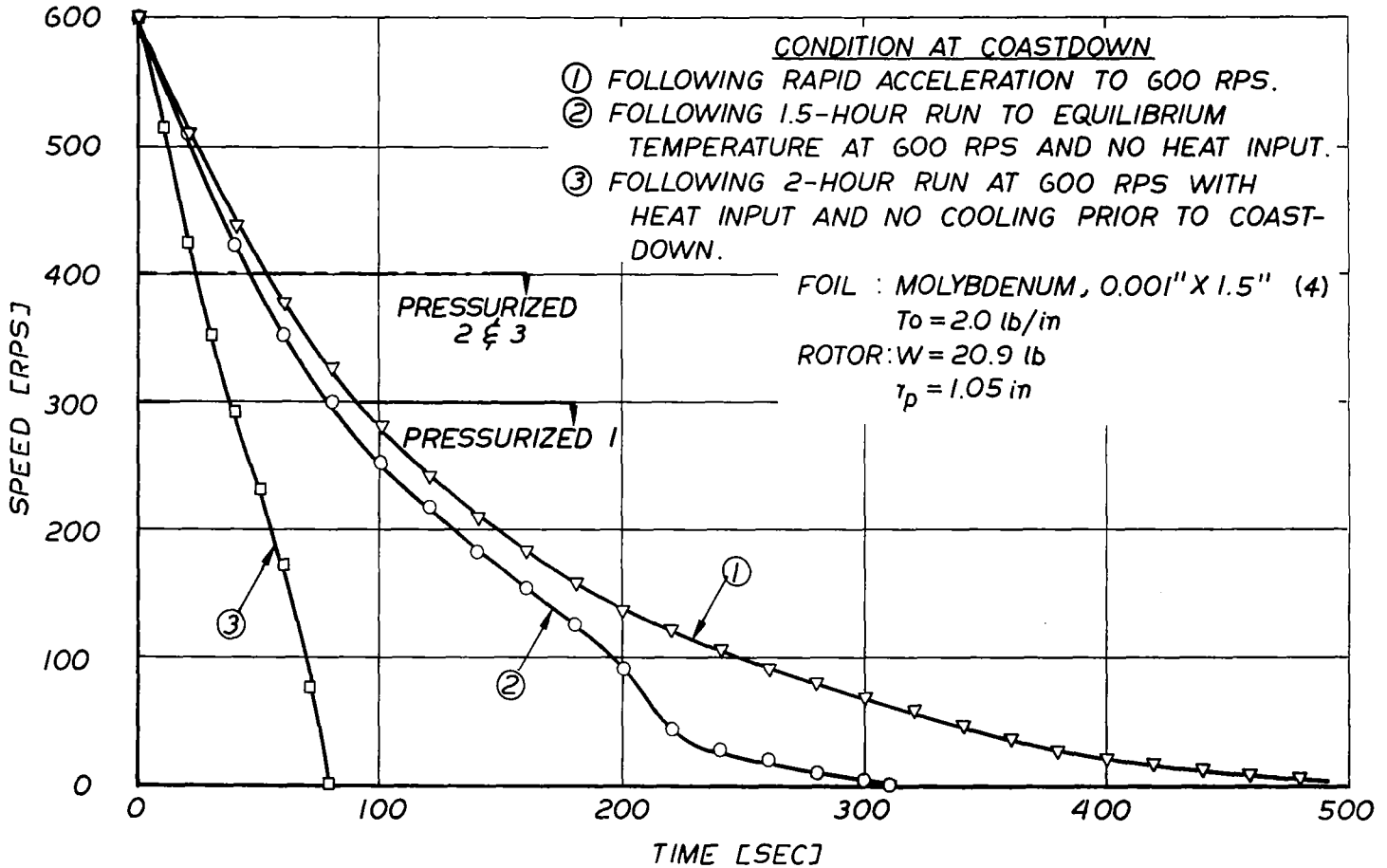

Fig. 26 Comparison of Coastdown Curves for 3 Initial Conditions (Rotor Vertical - Molybdenum Foils; r_p = radius of gyration)

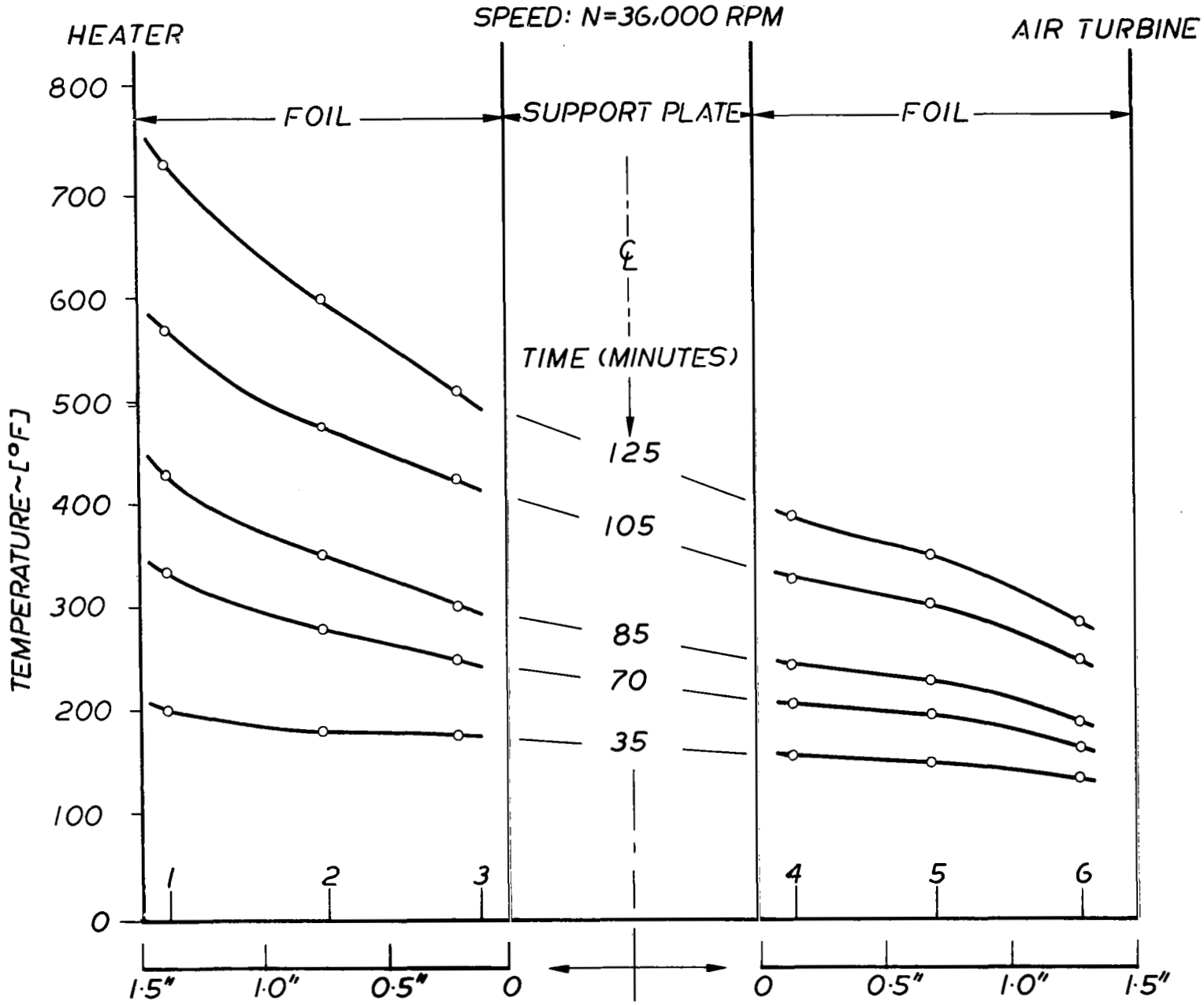

Fig. 27 Variation of Foil Temperature Along Rotor Axis
(Rotor Vertical - Molybdenum Foils)

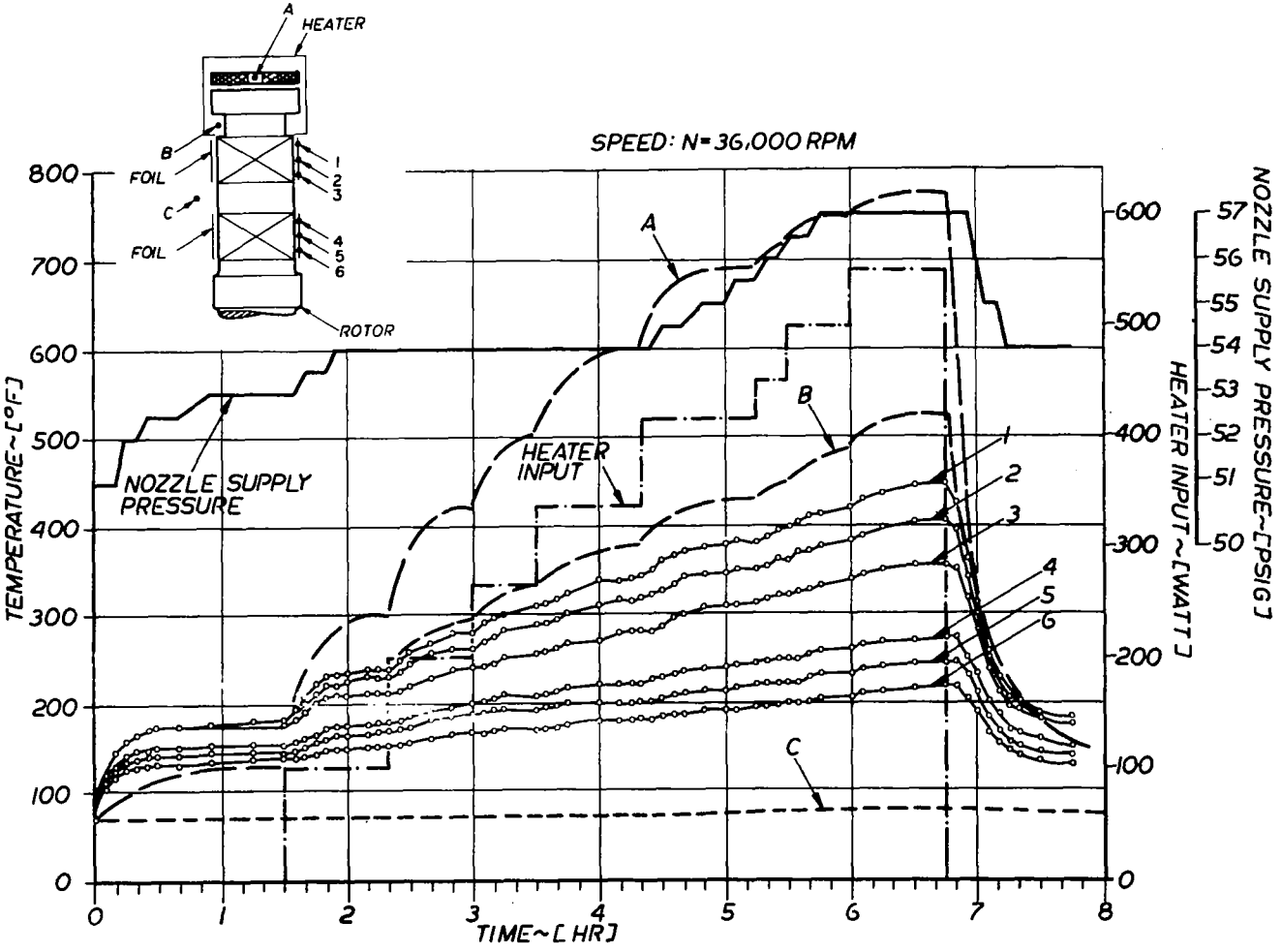

Fig. 28 Temperature Record of Heating Cycle (Rotor Vertical - 3 Molybdenum and 1 Inconel-600 Foil)

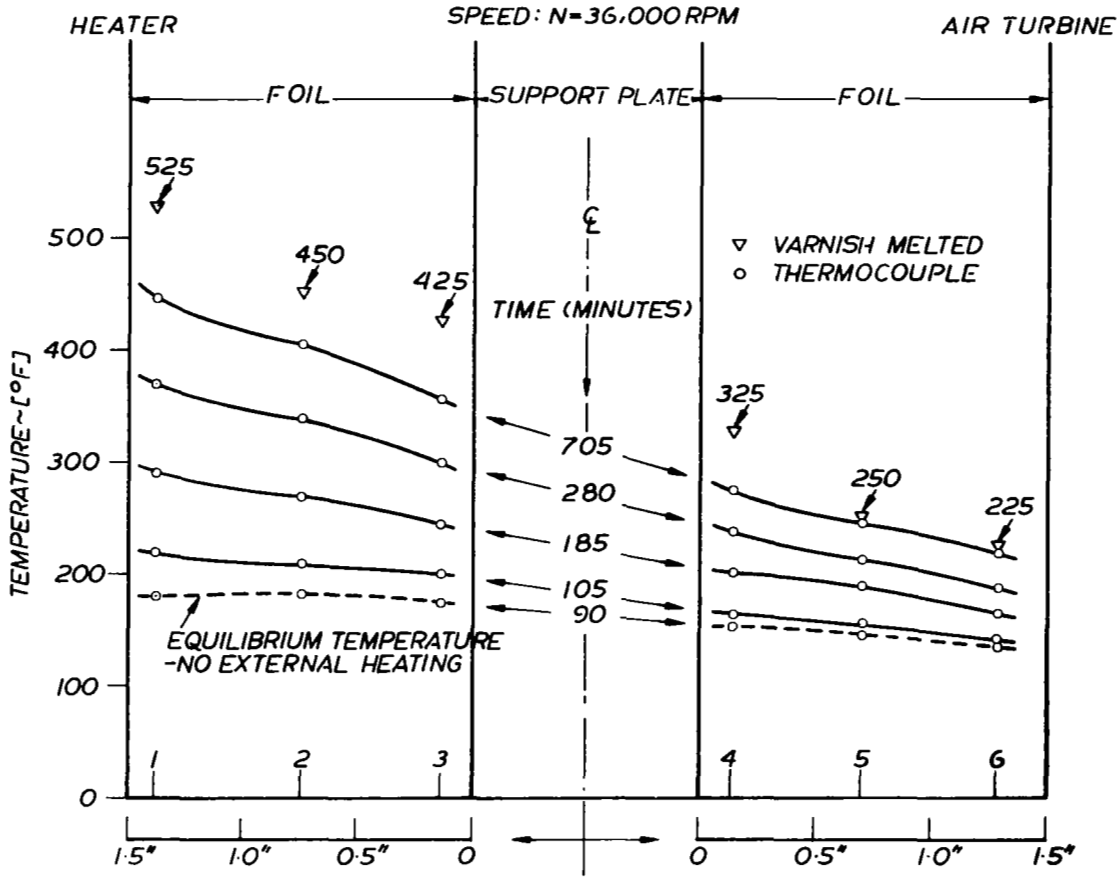

Fig. 29 Variation of Foil Temperature Along Rotor Axis (Rotor Vertical - 3 Molybdenum and 1 Inconel-600 Foil)

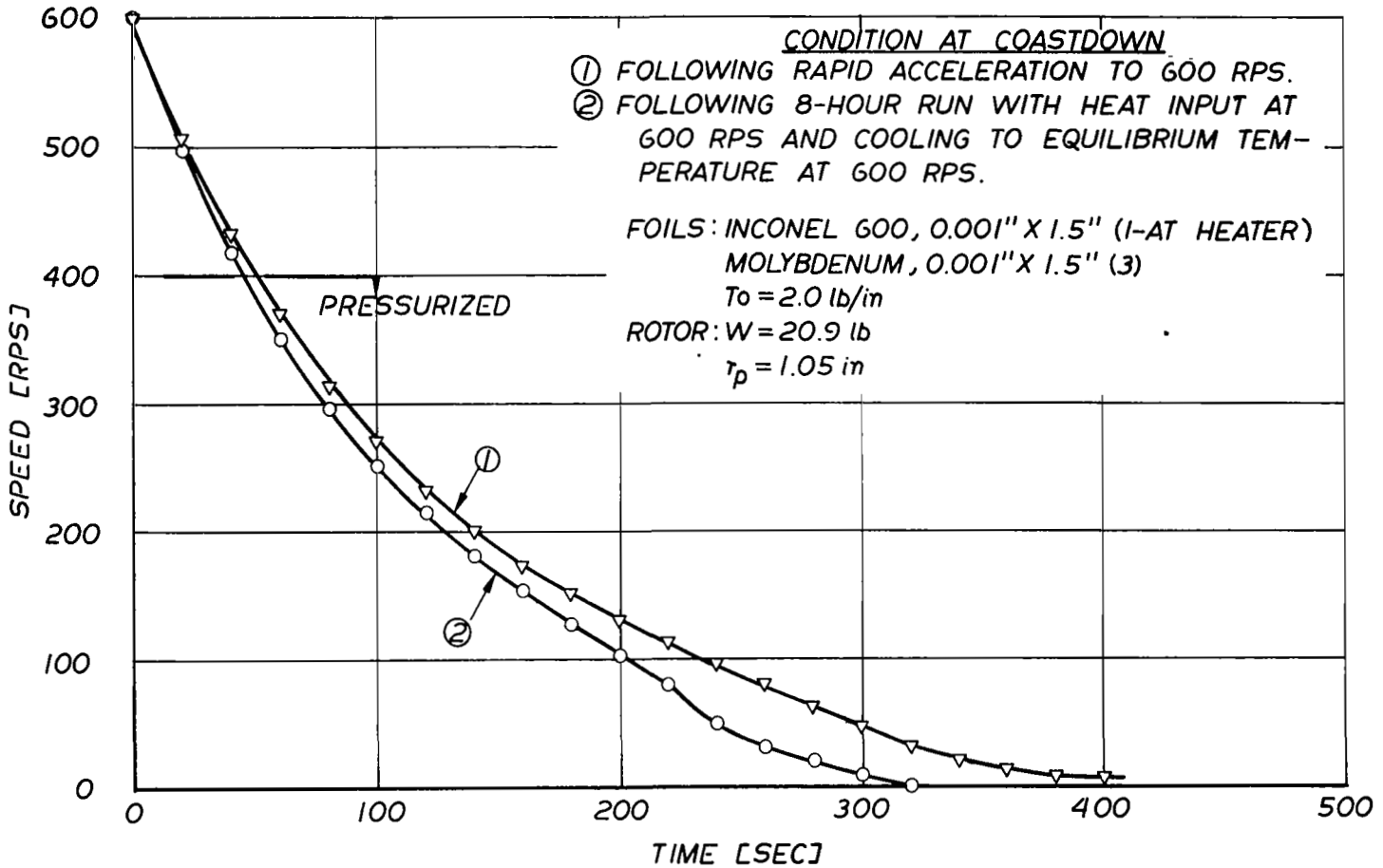

Fig. 30 Comparison of Coastdown Curves for 2 Initial Conditions (Rotor Vertical - 3 Molybdenum and 1 Inconel-600 Foil; r_p - radius of gyration)

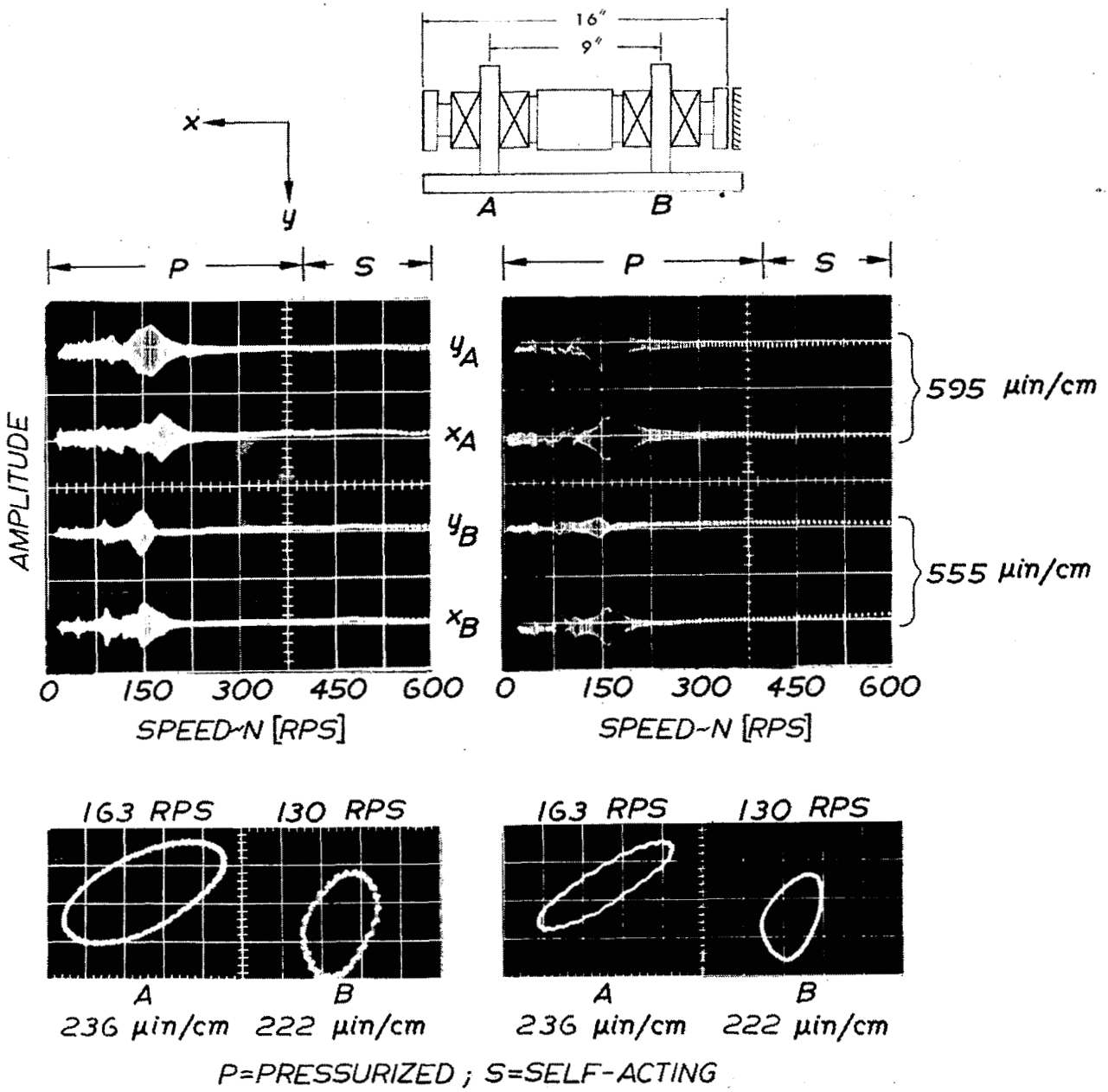

Fig. 31 Scans of Rotor Response During Coastdown
(Rotor Vertical - 3 Molybdenum and
1 Inconnel-600 Foil)

I. On Reaching Equilibrium Temperature After 1.5-Hour Run at 600 RPS with no Heat Input (left)

II. After Cooling at 600 RPS and Following 8-Hour Run with Heat Input at 600 RPS (right)

high-speed orbits were negligibly small and no additional resonances have been observed. It would appear, therefore, that high-speed operation is also possible in the pressurized mode, and with gap width the order of 0.002 inch.

4.5 Wipe-Wear Characteristics

The "forgiving" nature of foil bearings was discussed in considerable detail in references [5, 6]. Indeed, our past and present experiences confirm the ability of the foil bearing to accommodate geometrical imperfections and misalignment, as well as thermal distortions. Furthermore, the assortment of dust and debris "digested" by the present foil bearings without any ill effects would have sufficed to cause failure in a host of conventional gas bearings.* Thus, regardless of surface compatibility of materials, the passage of foreign particles is facilitated by the ability of the foil to deflect and to conform locally. Finally, since closure of the gap involves the entire region of wrap, rather than a line along the minimum clearance of a rigid bearing, contact is progressive and the load more uniformly distributed among a multiplicity of asperities. Hence, wiping and burnishing takes place - especially with suitably coupled materials - rather than ploughing, galling and scoring.

The same set of foils was used throughout the entire set of experiments described in the preceding sections, with the exception of replacing the molybdenum foil adjacent to the heater by an Inconel-600 foil after the first non-isothermal test run.

The foils were removed after the conclusion of tests at elevated temperatures for inspection of bearing surfaces. The state of the journal

*We have taken no precautions, for example, to prevent airborne particles, carried by the whirlwind of turbine-air discharge, from getting into the foil-bearing entrance zones and into the gaps. No special precautions were taken during assembly, mounting of the thermocouples and heating enclosure, or with respect to filtration of the air supply.

surfaces is depicted in Fig. 32, in which the upper photograph corresponds to the heated end of the rotor. The state of 12 molybdenum and of 3 Inconel 600 foil sectors, corresponding to the 60-degree regions of wrap, are presented in Fig. 33. The upper two rows (Inconel and molybdenum) contain foil sectors adjacent to the heater, and the last row contains sectors adjacent to the thrust bearing.

Significant surface contact occurred only in the hottest part of the bearing. The most pronounced wear track on the journal was along the outboard row of orifices. Contact pressure was due mainly to rapid contraction of the molybdenum foil along the row of cooling air jets during coastdown of the rotor. Despite rapid cooling of the molybdenum foil from approximately 800° F, the surface damage of foil segments A_{11}, A_{12} and A_{13} was slight and their condition was hardly inferior to that of the Inconel-600 sectors $\overline{A}_{11}$, $\overline{A}_{12}$ and $\overline{A}_{13}$, which had not been exposed to coastdown of the rotor at elevated journal temperature.* The remaining foil sectors displayed only minor wear marks, to the extent that borderlines between the regions of wrap and the adjacent foil areas were difficult to distinguish. The dark circular spots on sectors A_{13} and A_{23} correspond to locations of thermocouples on the opposite foil surface and do not represent a wear pattern.

4.6 Response to Unidirectional Excitation by a Vibrator (Shake-Table)

The experiments pertinent to the response of the system to rotating imbalance furnished no information with respect to resonances in the self-acting mode. These resonances, since they occur in a frequency interval adjacent to the resonant bandwidth in the pressurized mode and

*Cooling of the massive journal is much slower than cooling of the foil. Effects of differential contraction can be minimized not only by suitable matching of coefficients of expansion, but also by preheating of the foil-lift air.

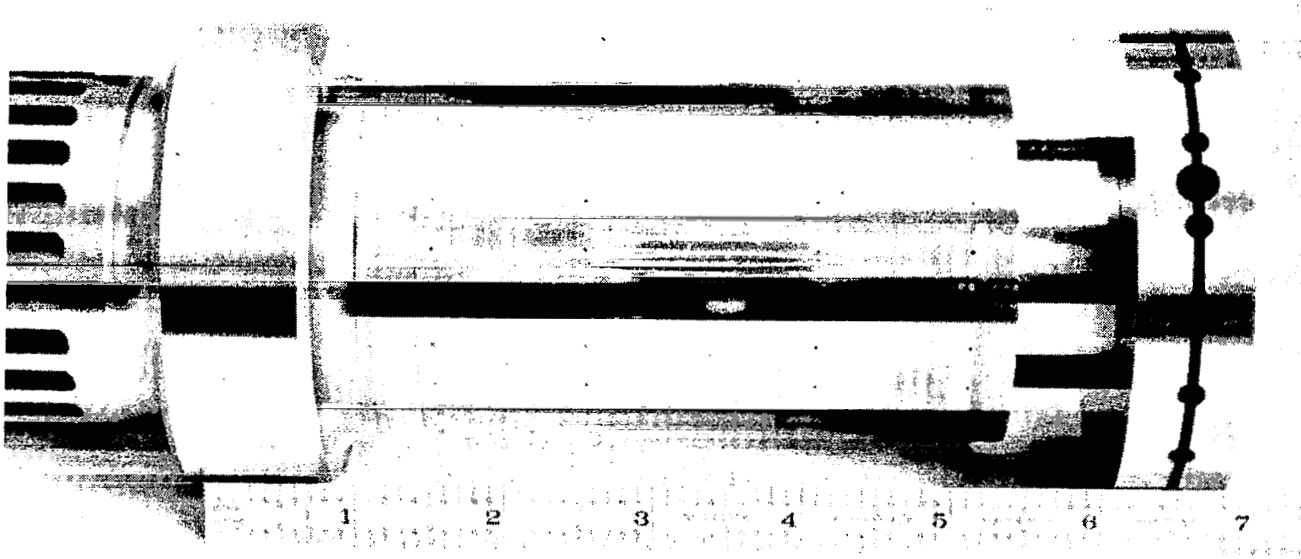

a) Heated End

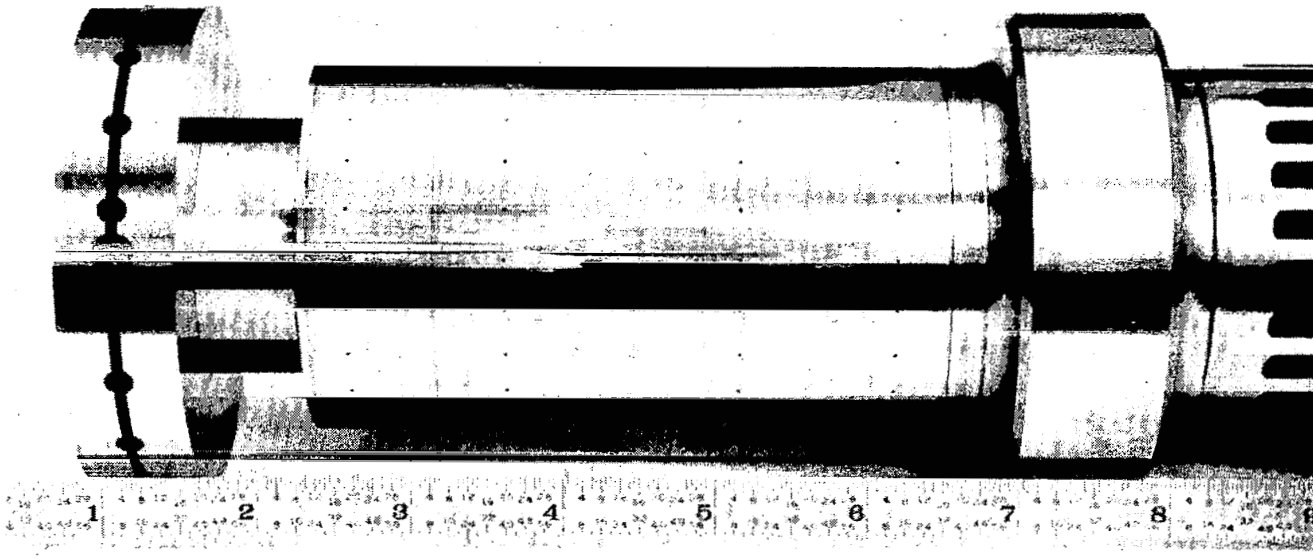

b) Cold End

Fig. 32 Wipe-Wear Traces on Rotor Journals

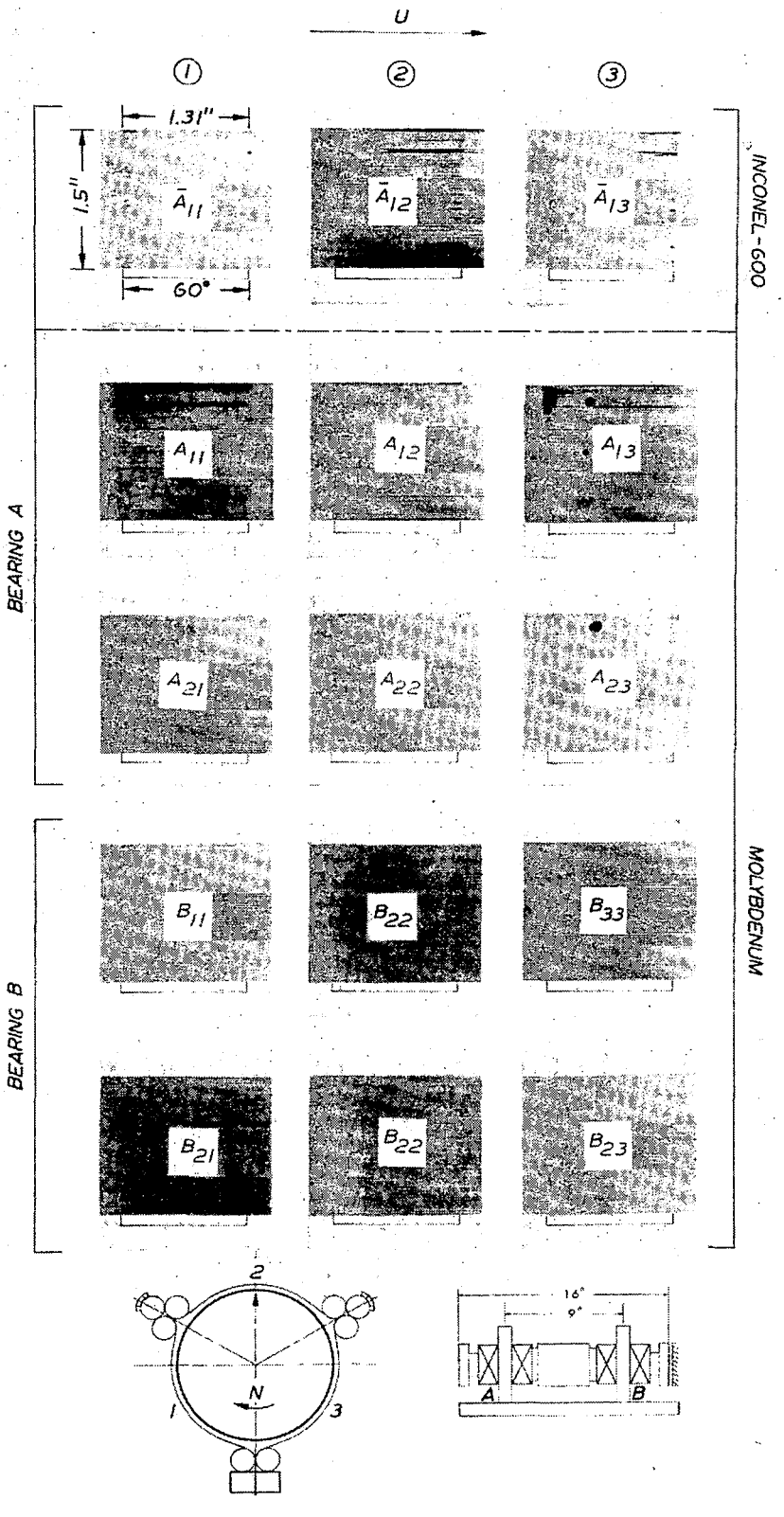

Fig. 33 Wipe-Wear Traces on Foil Sectors

below the transition speed to the self-acting mode, could not be consequently observed in the course of previous experiments.

The purpose of the shake-table experiments was to determine various performance characteristics of the rotor when subjected to periodic unidirectional excitation. A view of the foil-bearing supported rotor, mounted on an oil-floated plate attached to the exciter head, is shown in Fig. 34 against the background of instrumentation associated with the vibration experiments. The excitation was imparted along a line perpendicular to both the rotor axis and the direction of gravity, that is perpendicular to the bisector of the unloaded foil segment.* All tests were conducted at the rated speed N = 36,000 RPM and the rotor was supported on 1 mil molybdenum foils, preloaded to approximately 2.0 lb/in.

Scans of response with increasing and decreasing frequency of excitation, in the range $25 < f_e < 1000$ CPS, are illustrated in the oscillograms of Fig. 35. Shown also are outputs of three accelerometers, the locations of which are indicated in the accompanying schematic diagram of the shake-table and the foil rotor system.** The scans are similar and show that resonances occurred in the narrow bandwidth centered approximately at $f_e \approx 185$ CPS. The maximum in-line excursions corresponding to an excitation level $G_x \approx 0.8$ (peak amplitude) were $(x_A)_{max} \approx 2100$ μin and $(x_B)_{max} \approx 1250$ μin. Typical orbits in the vicinity of these maximum excursions are shown in Fig. 36 and the frequencies of excitation at which

*In a set of similar experiments described in references [5] and [6], the direction of gravity coincided with the axis of rotation and excitation was along a bisector passing through the foil lock.

**G_x was the controlling accelerometer, with the output of G'_x and G_y used to assess yawing and pitching of the vibrating support-plate. The plate was floated on a thin film of oil, on a granite table, and was bolted to the exciter head. No other constraints were furnished. The plate translated parallel to itself up to approximately 400 CPS. Thereafter, various structural resonances occurred and the motion was more complex.

these maxima occurred were approximately 170 CPS and 200 CPS. The motion in the resonant region was quasi-cylindrical, so that the traces of the in-line probe outputs in the second oscillogram of Fig. 36 are nearly in-phase and do not differ greatly in amplitude.

The motion of the rotor in the monitoring plane A, at various frequencies of excitation, is illustrated in Fig. 37. The reader will note that the displacement was nearly collinear with the excitation, changing into a narrow quasi-elliptical orbit at resonance. The timebase oscillogram in Fig. 37 shows the phase shift between in-line acceleration and in-line displacement in passing through resonance. The overall collinearity of excitation and displacement can also be noted in the first oscillogram of Fig. 38. The latter shows that at N = 600 RPS and f_e = 300 CPS, the amplitude of motion increases nearly linearly at a rate of approximately 175 μin/g in the range of excitation 1 g $\leq G_x \leq$ 5 g. The second oscillogram shows the sinusoidal waveforms of the G_x accelerometer output. We note in passing that, unlike in other types of fluid-film bearings, excitation at $f_e = N/2$ causes no loss of load capacity and an associated growth of amplitude of motion.

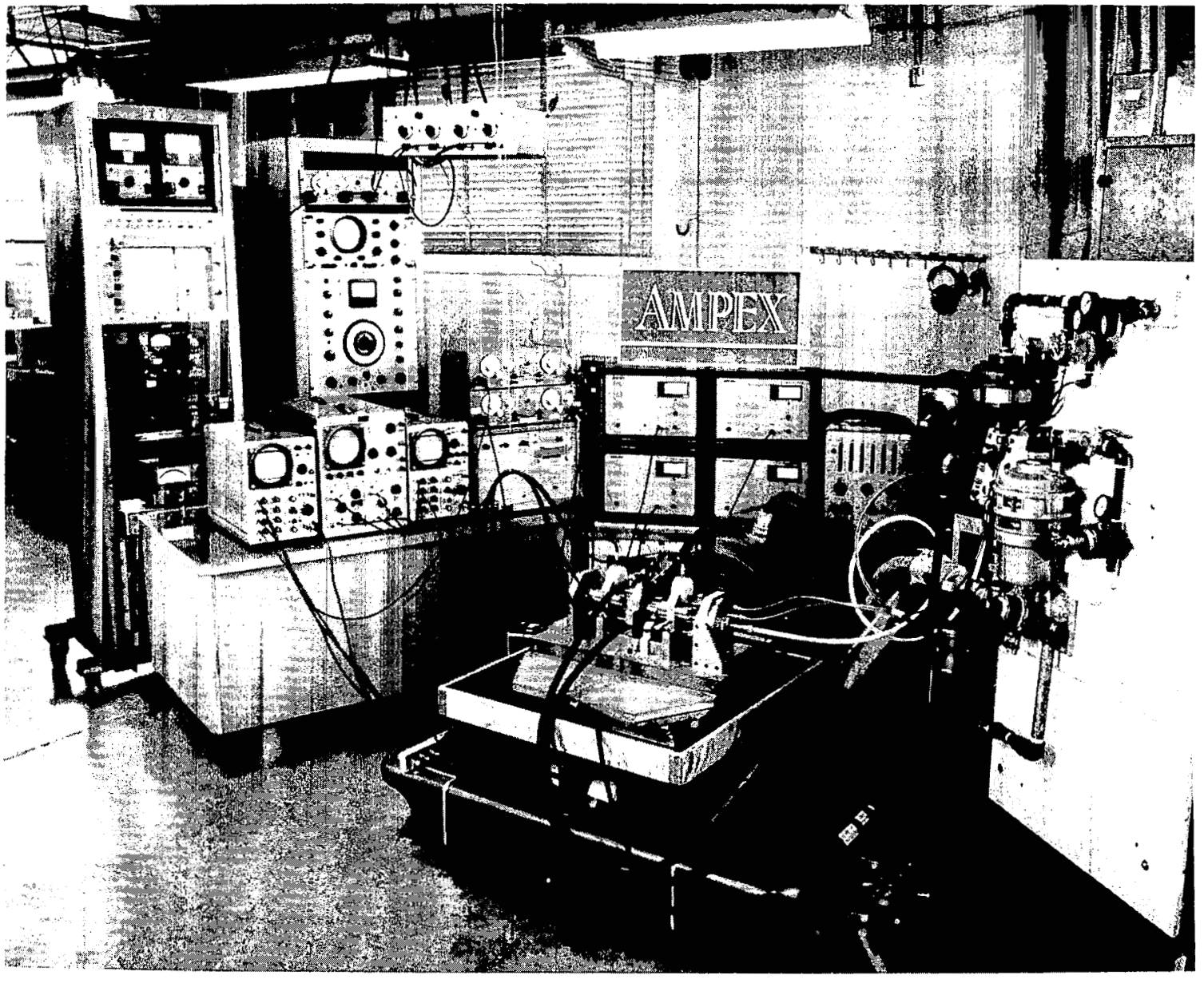

Fig. 34 View of Foil-Bearing Supported Rotor, Vibrator and Instrumentation

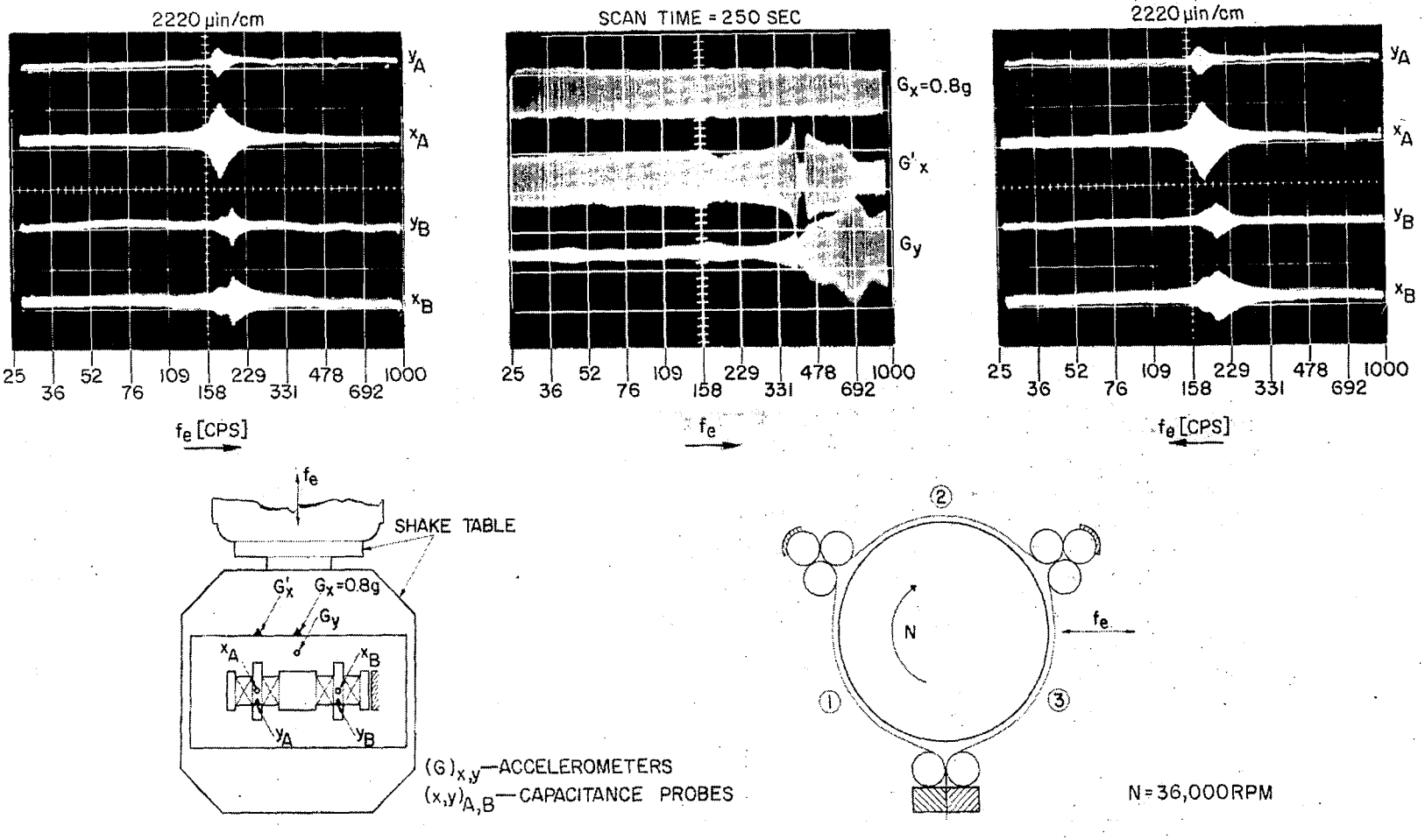

Fig. 35 Scan of Response to Unidirectional Excitation
(Horizontal Attitude; N = 36,000 RPM; G_x = 0.8 g)

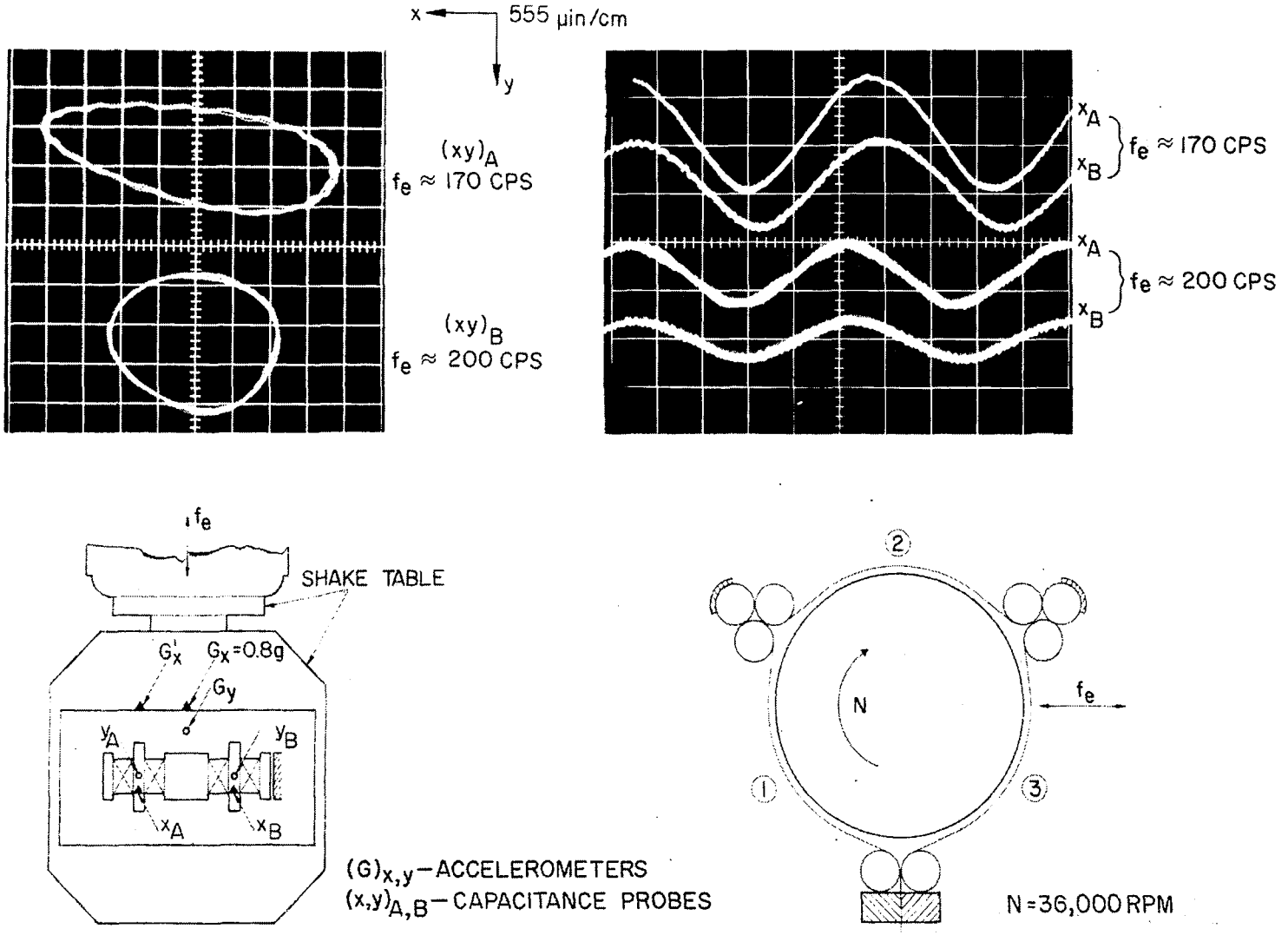

Fig. 36 Motion of Rotor in Region of Resonances
(Horizontal Attitude; N = 36, 000 RPM;
G_x = 0. 8 g)

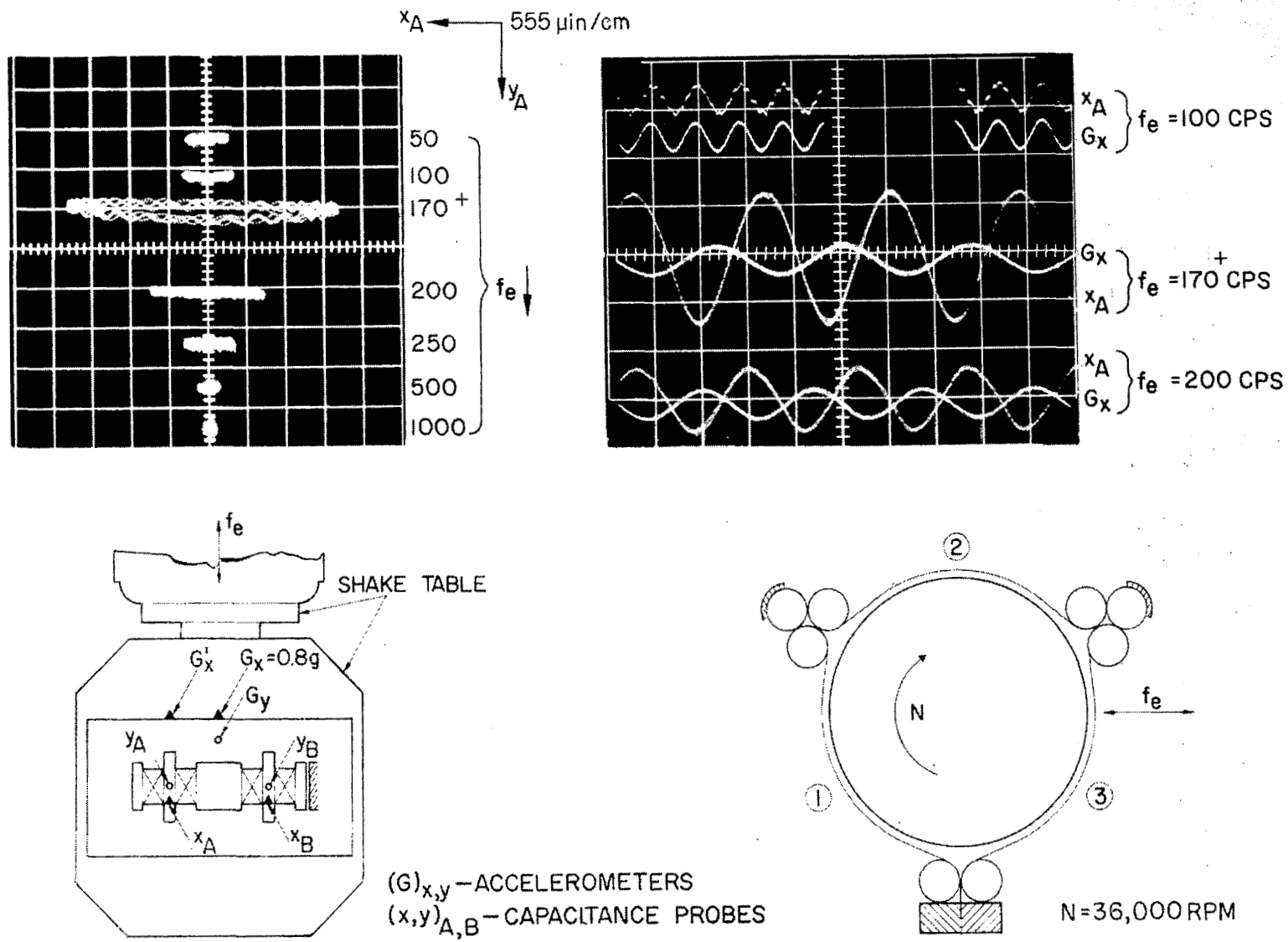

Fig. 37 Motion of Rotor at Various Frequencies of Excitation
(Horizontal Attitude; N = 36,000 RPM; G_x = 0.8 g)

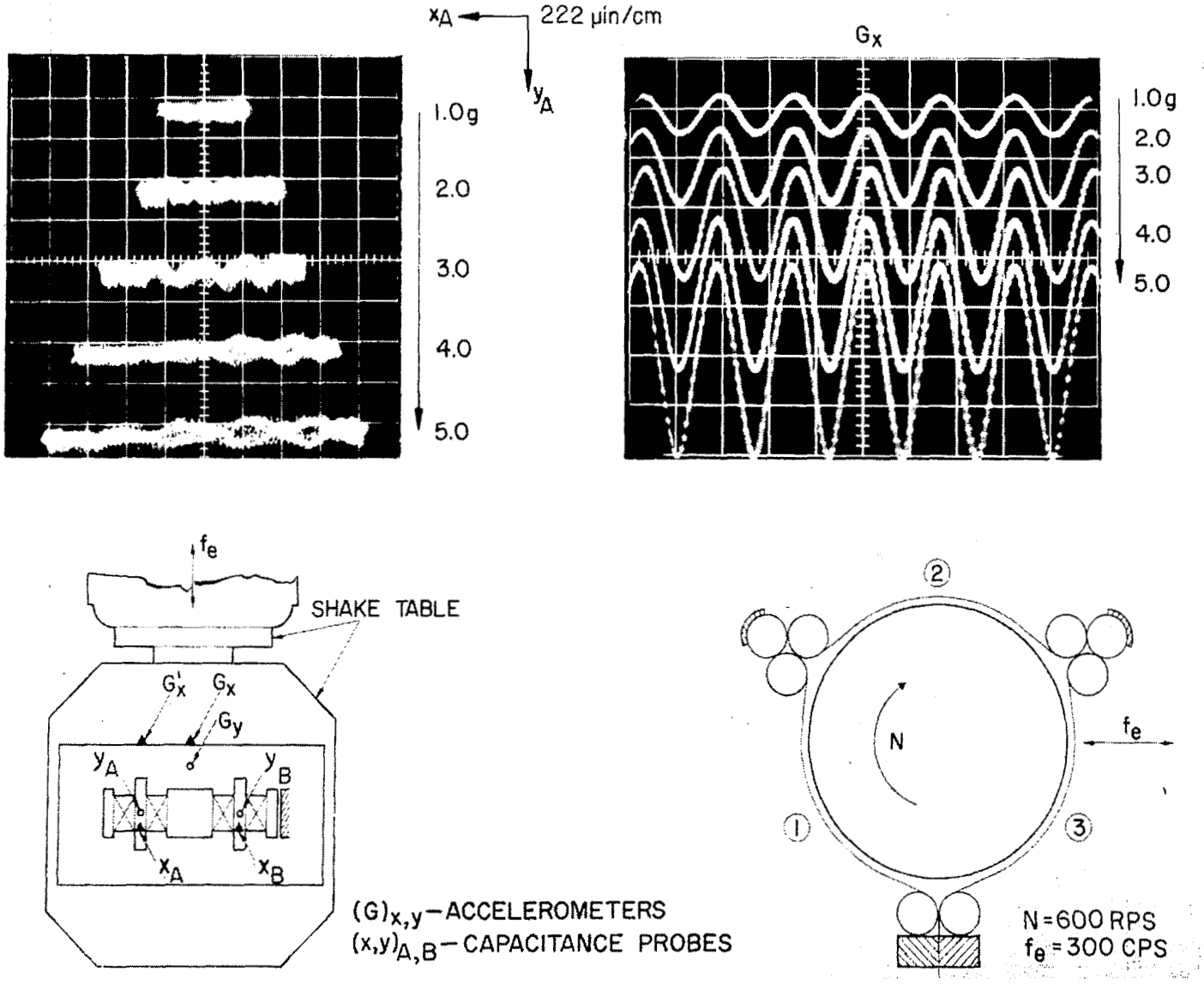

Fig. 38 Response of Rotor at Variable Level of Excitation (Horizontal Attitude; N = 600 RPS; f_e = 300 CPS; $1 \leq G_x \leq 5$ g)

5.0 CONCLUSIONS AND RECOMMENDATIONS

The experimental results presented in the preceding sections pertain to a 21-pound rotor, supported by foil bearings and operated stably in both the vertical and horizontal attitudes at speeds up to 50,000 RPM. The mass, the polar and transverse moments of inertia, the bearing span and the bearing stiffness of the simulator matched closely those of a Brayton Cycle Turbo-Alternator undergoing development under the sponsorship of NASA [7].

Of the advantages of foil bearings listed below, all have been substantiated by extensive tests in the course of the present and preceding studies:

a) Freedom form self-excited vibrations, commonly referred to in literature as "half-frequency" or "fractional-frequency" whirl. This consideration is particularly important in the state of weightlessness, in which instability of gas-bearing supported rotors is most likely to occur [8]

b) Excitation at frequency equal to half the speed of rotation causes no loss of load capacity. The half-speed danger point characterizes most rigid, fluid-film bearings, but is absent in foil bearings.

c) Motion of the journal is not constrained by the narrow confines of the clearance circle. Both foil and journal can displace while maintaining the lubricating film. Rotor excursions several times the order of clearance of a conventional gas bearing can thus be accommodated.

d) The foil bearing is extremely forgiving of foreign particles. It accommodates geometrical imperfections, misalignments and thermal distortions, and it is characterized by excellent wipe-wear characteristics.

e) Manufacture is simple and no stringent requirements exist with regard to dimensional accuracy and roundness. The performance of foil bearings appears to be quite insensitive to large variations of various bearing parameters and operation can be maintained under conditions which could not be tolerated with other types of bearings.

At the present state of this relatively new bearing art, possible disadvantages of foil bearings, in comparison with other types of bearings, may be the following:

a) Relatively low stiffness (typically 15,000 lb/in for a 2.5-inch diameter, 1.5-inch long bearing).

b) Relatively greater journal-length requirement.

c) More elaborate pressurization system for starting.

The foil bearing is not intended to compete in stiffness with other types of bearings, although an appreciable increase of stiffness can be achieved above the value attained with the experimental bearings. The practicality of gas-lubricated foil bearings has been demonstrated and the adoption of this method of support for high-speed turbomachinery is recommended. While incorporation of the present foil-bearing configuration in the overall design of turbomachines is in itself a practical proposition, further development is recommended. In order to capitalize fully on the potential of foil bearings, future development should be concentrated on problems related to improved and novel methods of foil mounting, reduction of journal length requirements, and simplification of starting methods. Concepts and devices to further the foregoing objectives are already under active consideration by personnel involved in the present project.

REFERENCES

1. L. Licht, "An Experimental Study of Elastohydrodynamic Lubrication of Foil Bearings," Part 1 - "Displacement in the Central Zone" and Part 2 - "Displacement in the Edge Zone," Journal of Lubrication Technology, Trans. ASME, Vol. 90, Ser. F, No. 1, January 1968, pp 199-220.

2. L. Licht, "An Experimental Study of Air-Lubricated Foils with Reference to Tape Transport in Magnetic Recording," Report No. 7, August 1966, Lubrication Research Laboratory, Columbia University, prepared under Contract Nonr-4259(14), Information Systems Branch, and Fluid Dynamics Branch, Office of Naval Research, Washington, D.C.

3. G. K. Fisher, J. L. Cherubim and O. Decker, "Some Static and Dynamic Characteristics of High-Speed Shaft Systems Operating with Gas-Lubricated Bearings," Trans. of the First International Symposium on Gas-Lubricated Bearings, October 1959, ACR-49, Office of Naval Research, Washington, D.C., pp 383-410.

4. A. Stahler and A. Huckabay, "Analysis, Design, Fabrication and Testing of a Foil Bearing Rotor Support System," Ampex Corporation RR 66-21, June 1966, prepared under Contract NASW 1221, NASA, Washington, D.C.

5. L. Licht and A. Eshel, "Study, Fabrication and Testing of a Foil-Bearing Rotor Support System," NASA CR-1157, November 1968, prepared by the Ampex Corporation under Contract NASW-1456, NASA, Washington, D.C.

6. L. Licht, "An Experimental Study of High-Speed Rotors Supported by Air-Lubricated Foil Bearings," Part 1 - "Rotation in Pressurized and Self-Acting Foil Bearings" and Part 2 - "Response to Impact and to Periodic Excitation," Journal of Lubrication Technology, Trans. ASME, Vol. 91, Ser. F, No. 3, July 1969,

7. "Brayton-Cycle Rotating Unit and Associated Research Hardware, AiResearch Manufacturing Company of Arizona, Progress Report APS-5227-R8, Contract NAS3-9427, March 1967.

8. W. A. Gross, "Gas Film Lubrication," John Wiley and Sons, Inc., New York, 1962, pp 334-362.

NASA-Langley, 1970 —— 15 E-5485